Deltares

Modelling seaweed cultivation on the Dutch continental shelf

Modelling seaweed cultivation on the Dutch continental shelf

Author(s)
Lauriane Vilmin
Luca van Duren

Modelling seaweed cultivation on the Dutch continental shelf

Client	Wageningen Marine Research
Contact	Mr. R.W. Nauta
Reference	This research project was carried out by Deltares at the request of Wageningen Marine Research and with funding from the “Maatschappelijk InnovatieProgramma” AF-16202 Seaweed for food and feed (Proseaweed), part of the research portfolio of Topsector Agri&food and the Dutch Ministry of Agriculture, Nature and Food Quality (project number BO-59-006-001)
Keywords	Seaweed cultivation, North Sea, primary production, nutrients, carrying capacity

Document control	
Version	1.0
Date	27-05-2021
Project nr.	11205769-002
Document ID	11205769-002-ZKS-0001
Pages	50
Classification	
Status	final

Author(s)

	Lauriane Vilmin	
	Luca van Duren	

Doc. version	Author	Reviewer	Approver	Publish
1.0	Lauriane Vilmin	Jos van Gils	Paul Saager	
	Luca van Duren			

Summary

While the seaweed *Saccharina latissima* is currently cultivated in the Netherlands at a small scale, there is a major drive towards increasing sustainable offshore cultivation. The incentive for multi-use of marine space notably motivates research on the opportunities and the risks of seaweed production in offshore windfarm (OWF) areas. Harvesting seaweed leads to the removal of nutrients from the ecosystem, which can subsequently affect phytoplankton primary production, the basis of the marine food web. An important question is: how much seaweed can be harvested without significant negative effects on the ecological functioning of the Dutch North Sea? Initial estimates did not consider other ecosystem functions and water currents. In the current project, we carry out a more thorough investigation of the environmental effects of seaweed cultivation in the Dutch North Sea, investigating spatial variability in ecosystem responses. We simulated several hypothetical scenarios and assessed the potential effects on regional and system scale parameters such as nutrients and phytoplankton primary production. We focus mainly on the interaction of seaweed and phytoplankton productivity with respect to nutrients and the effect of size, location and distribution of seaweed farms on seaweed production and its environmental effects.

We therefore integrated a module simulating seaweed nutrient uptake, growth and mortality dynamics into a fully coupled 3D hydrodynamic-water quality model of the North Sea (3D DCSM-FM). 3D DCSM-FM was developed in recent years as part of Deltares' strategic research and tested in the WOZEP programme (offshore wind ecological programme from the Dutch government) to assess the physical effects of offshore turbines on phytoplankton primary production in the North Sea. The seaweed module, based on a published model for growth of *S. latissima* off the Norwegian coast, was extended to include phosphorus uptake dynamics. Nutrient uptake parameters were based on recent lab analysis of *S. latissima* cultivated off the Dutch coast. Besides a reference run, without seaweed cultivation, we ran different hypothetical cultivation scenarios over a production year (September 2016–September 2017), and compared the resulting nutrient concentration and phytoplankton primary production fields. The scenarios included extreme upscaling, to 25% of all designated OWF areas (i.e. 790 km^2), as well as tests of smaller-scale farming (down to 0.8 km^2 plots) at various locations.

The model results showed that the offshore locations seem to be slightly more productive seaweed cultivation locations than those closer to the coast, and that it is beneficial to split the cultivation area into small plots. Growth of total seaweed biomass is mainly driven by temperature and light, since the fronds do not run out of reserves before harvest. For all tested scenarios and at all locations, a seaweed production of 0.75 to 1 $kgDW/m^2$ could be reached. Upscaling of seaweed production to 25% of all Dutch designated OWF areas would have a strong impact on the ecology, with local decreases in spring phytoplankton production as high as 30%. The effect on nutrient concentrations and phytoplankton primary production is directly related to the size of the farms. Small scale farms (plots of ~0.8 km^2) individually have a limited impact in terms of decrease in nutrients and primary phytoplankton production (< 1% at all tested locations). The effects of larger farms can extend far in the direction of the current. For example, seaweed cultivation over 25% of a ~100 km^2 area at the OWF Borssele leads to a decrease in spring primary production >1% over more than 3,000 km^2, all the way North from the Dutch Wadden Islands. Therefore, the location of seaweed farms with respect to each other is also an important factor to account for when upscaling seaweed production in the North Sea. Having seaweed farms within each other's nutrient footprint will have little influence on the integrated effect over the entire ecosystem, as long as local effects are such that seaweed nutrient reserves do not get depleted. However, placing a new seaweed farm in the area of influence of another one will lead to higher local reductions in nutrient concentrations and phytoplankton primary production.

Future potential improvements to the model have been identified. To refine the model's assessments in terms of seaweed production and effect on the environment, and before it can be used for any regulation purposes, it is crucial to calibrate and validate seaweed dynamics on field data, as soon as these become available, and to include the effect of dense seaweed cultures on the flow. When these improvements are carried out, this model could be used to refine our estimates of the ecological carrying capacity of the Dutch North Sea for seaweed cultivation.

Contents

1 Introduction

1.1 Background

There is a major drive in the Netherlands towards sustainable offshore cultivation of seaweed. Seaweed production is currently relatively small scale and restricted to kelp species, such as *Saccharina latissima*. In future several other species with high market potential will be considered. Offshore cultivation has several technical and logistic challenges, as well as advantages. The challenges are concerned with offshore conditions, risks of dislodgement, restricted operational windows and questions about potential yields. The advantages are utilisation of offshore resources, potential reduction of eutrophication of offshore locations, more available space than in nearshore environments and potential co-use of marine space within wind farms. The positive impact of reducing eutrophication strongly depend on the trophic status of the local system. Eutrophication in the North Sea is largely restricted to coastal waters under the direct influence of freshwater run-off from land (Ærtebjerg et al. 2001), hence positive effects on eutrophication may still be present in areas under the influence of the Rhine plume but will be negligible further offshore.

One of the main questions for offshore production is the ecological carrying capacity, i.e. the amount of seaweed that can be harvested without significant negative effects on the ecological functioning of the North Sea. In the mid-20th century excessive run-off of nutrients from land (mainly from agriculture) led to eutrophication of coastal waters with negative effects such as harmful algal blooms and low oxygen levels in stratified areas (Emeis et al. 2015). In recent years, mainly due to measures under the Water Framework Directive (WFD) nutrient loads (particularly phosphate) have been reduced and we are starting to see improvements in water quality (Prins, Desmit, and Baretta-Bekker 2012). Harvesting seaweed means removing nutrients from the system. As the North Sea system is currently still slightly more eutrophic than desirable, the initial effects are likely beneficial. However, if seaweed cultivation is scaled up to levels that are commercially profitable, there is a risk of overexploitation. Long before the *production carrying capacity* is reached (i.e. the level of production where more production would start to see less economic return, as nutrient levels are too far depleted) it is likely that *ecological carrying capacity* is transgressed. Estimating production carrying capacity is a relatively easy task, establishing ecological carrying capacity is much more complex. In principle any extraction of nutrients will have some effect. Which effect is *significant* on a regional or on a system level, is not straightforward.

There are some initial estimates available, based on fairly coarse mass balance calculations (Van den Boogaart et al. 2020; Van Duren et al. 2019). These do take other ecosystem functions into account, but only on a very abstract level. They are mainly based on nutrient concentrations and do not take ambient currents into account.

The current project involves a more thorough investigation of the effects of seaweed cultivation in the North Sea, not just for the system as a whole, but also in different subregions. This work is based on available suitable ecosystem models that take local nutrient inputs as well as local residence times of water into account. Particularly the competition between seaweed growth and the ambient phytoplankton is investigated. Primary production from phytoplankton is the basis of the marine food web. In this project the effects of changes in phytoplankton production on higher trophic levels are not specifically considered.

1.2 Goal of this study

The assignment focusses on two distinct main questions:
1. The interaction of seaweed and phytoplankton productivity with respect to nutrients;
2. The relation between size, location and distribution of seaweed farms with respect to phytoplankton primary production and seaweed production.

In this study we present a few hypothetical scenarios and assess the potential effects of seaweed cultivation layouts on regional and system scale trophic state parameters. We focus on phytoplankton primary production, as the keystone of the ecosystem. Nutrient concentrations are investigated as well, essentially to support our understanding of changes in primary production. These results constitute a step towards a refined assessment of ecological carrying capacity for seaweed cultivation in the North Sea.

2 Methods

Hydrodynamics, water quality processes and seaweed dynamics are computed using the D-Flow Flexible Mesh (D-Flow FM) component from the Delft 3D Flexible Mesh Suite (Zijl, Veenstra, and Groenenboom 2018; Zijl, Groenenboom, and Laan 2020). Water quality processes are simulated with the D-Water Quality module, fully integrated within D-Flow FM (i.e. tightly coupled hydrodynamics and water quality). The scenarios are run using a version of the 3D Dutch Continental Shelf Model – Flexible Mesh (3D DCSM-FM) which has been developed and validated within the WOZEP project (Zijl et al. 2021).

2.1 The North Sea 3D DCSM-FM model

3D DCSM-FM was developed in recent years as part of Deltares' strategic research. The model covers the Northwest European Continental Shelf, including the North Sea and adjacent shallow seas, such as the Wadden Sea (Figure 2.1). The model grid is coarser near the open boundaries and in deep waters (approximatively 4 by 4 nautical miles) and the resolution increases toward the shallower waters and in the Southern North Sea to 0.5 by 0.5 nautical miles (~900 m). The water column is divided into a fixed number of 20 layers over the entire domain (sigma-layer approach). These layers have a uniform thickness of 5% of the total water depth. For additional model testing, and to reduce computation time, a coarse-grid version of the model (4 nautical mile resolution over the entire domain) was also applied, using the same settings as the fine-grid model described herein. Its results in terms of water quality were shown within the WOZEP project to be very similar to the coarse grid ones in the offshore regions.

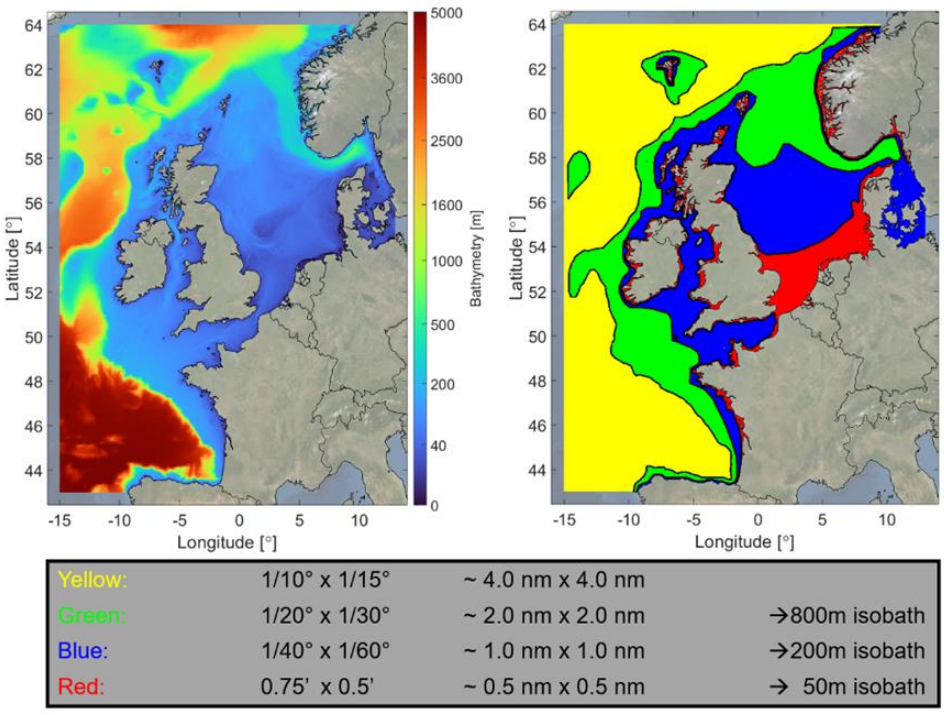

Figure 2.1: Bathymetry and grid cell size of the 3D DCSM-FM model.

3D DCSM-FM computes water levels (tide and surge) as well as heat and salinity. Bed friction is calculated using a spatially varying Manning roughness coefficient, adjusted to obtain an optimal water level representation.

2.2 Representation of biogeochemical processes

Biogeochemical processes are simulated using the D-Water Quality module. Process representations are selected from the D-Water Quality Process Library (Deltares 2021). Processes were parameterised as in the GEM model (Blauw et al. 2009), which has been applied in earlier ecosystem projects focused on the North and Wadden seas, such as the "MER zandwinning Noordzee" project for Rijkwaterstaat (van der Kaaij et al. 2017). A new seaweed module (MALG), developed within the IMPAQT H2020 project (Schueder and van Duren 2019) was plugged into D-Water Quality to simulate the dynamics of *S. latissima*, and run simultaneously to all other biogeochemical processes. All water quality substances included in the model are listed in Table 2.1.

Table 2.1: Description of simulated water quality state variables.

Model state variable	Description	Unit	Active*
OXY	Dissolved oxygen	mg/L	✓
NH4	Ammonium	mgN/L	✓
NO3	Nitrate	mgN/L	✓
PO4	Phosphate	mgP/L	✓
Si	Silica	mgSi/L	✓
Opal	Biogenic silica	mgSi/L	✓
POC	Particulate Organic Carbon	mgC/L	✓
PON	Particulate Organic Nitrogen	mgN/L	✓
POP	Particulate Organic Phosphorus	mgP/L	✓
DIAT_X, DINO_X, FLAG_X, Phae_X (X=E, N, P)	Diatoms, dinoflagellates, flagellates and *Phaeocystis* (energy-, nitrogen- and phosphorus-limited)	mgC/L	✓
DetCS	Detrital carbon in sediment layer	gC/m^2	
DetNS	Detrital nitrogen in sediment layer	gN/m^2	
DetPS	Detrital phosphorus in sediment layer	gP/m^2	
DetSiS	Detrital silica in sediment layer	gSi/m^2	
Mussel_V	Structural biomass of mussels	gC/m^2	
Mussel_E	Energy reserves of mussels	gC/m^2	
Mussel_R	Reproductive biomass of mussels	gC/m^2	
Ensis_V	Structural biomass of *Ensis*	gC/m^2	
Ensis_E	Energy reserves of *Ensis*	gC/m^2	
Ensis_R	Reproductive biomass of *Ensis*	gC/m^2	
MALS	Seaweed structural mass	gDW/m^2	
MALC	Seaweed carbon reserves	gC/m^2	
MALN	Seaweed nitrogen reserves	gC/m^2	
MALP	Seaweed phosphorus reserves	gC/m^2	

* "Active substances" are those that can be transported by advection/diffusion processes

The water quality model simulates the cycles of major nutrients (nitrogen, phosphorus and silica, herein noted N, P and Si), organic carbon (C) and dissolved oxygen (O_2). Simulated processes comprise (Figure 2.2):

- Phytoplankton photosynthesis and associated uptake of nutrients and O_2 production that depend on the light climate;
- Vertical attenuation of photosynthetically active solar radiation;
- Phytoplankton respiration and mortality resulting in the release of nutrients and the consumption of O_2;
- Metabolism of grazers on the seafloor (blue mussels in the Wadden Sea and *Ensis* elsewhere);
- Mineralization of organic matter in the water column and in the sediment and associated O_2 consumption;
- Dissolution of biogenic silica in the water column and in the sediment;
- Settling of organic matter and phytoplankton and burial of detrital organic matter;
- Nitrification;
- Denitrification in the water column and in the sediment;
- Atmospheric deposition of NH4 and NO3;
- Oxygen re-aeration at the water surface;
- Seaweed carbon and nutrient uptake and growth dynamics.

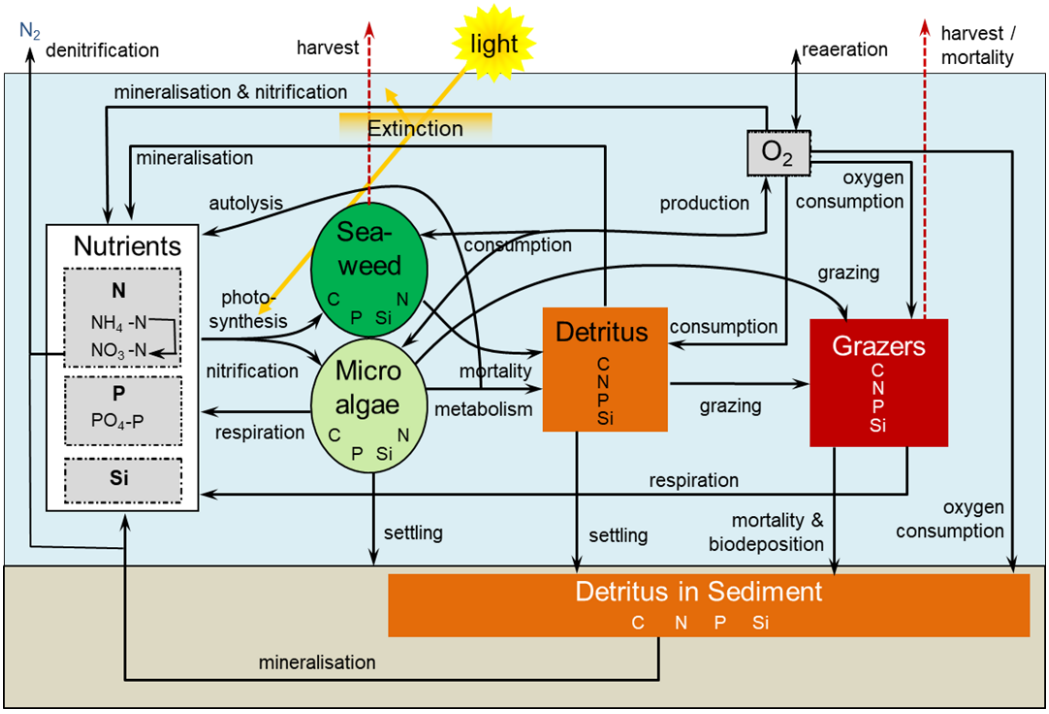

Figure 2.2: Scheme of variables and processes simulated within the ProSeaweed project.

Phytoplankton dynamics (primary production, respiration and mortality) are simulated using the BLOOM module (Los and Brinkman 1988; Los, Villars, and der Tol 2008). BLOOM represents competition and adaptation of phytoplankton to nutrient or light-limiting conditions. Here, four species groups are simulated: marine diatoms, flagellates, dinoflagellates and *Phaeocystis*. For each of these groups, three ecotypes are defined to account for adaptation to changing environmental conditions:

- an energy type ("_E"), with relatively high growth rate, low mortality rate and high N:C and P:C ratio, and higher chlorophyll content;
- a nitrogen type ("_N"), with typically lower internal N:C ratio, lower maximum growth rate, higher mortality rate, higher settling velocity and lower chlorophyll-a content;
- a phosphorus type ("_P"), similar to the nitrogen type with typically lower internal P:C ratio.

Species composition is calculated using linear programming to maximize the total net production of the whole phytoplankton community, depending on the prevailing conditions, and therefore does not require any initialization or boundary conditions for the simulated phytoplankton. This implies that fast-growing phytoplankton (energy type) dominate in situations where light and nutrient resources are abundant, while slow-growing, efficient phytoplankton species become dominant when resources become limited (Blauw et al. 2009). While all other water quality processes are run simultaneously at each user-defined time step, BLOOM is designed to represent phytoplankton dynamics with a 24h time step. BLOOM is computed at the start of each day, before all other processes.

Grazer dynamics are simulated with the DEBGRZ module (Troost et al. 2010), based on the Dynamic Energy Budget (DEB) theory (Kooijman 2010). In the present model, DEBGRZ is used to model blue mussel beds (*Mytilus edulis*) in the Wadden Sea and American razor clams (*Ensis leei*) in the North Sea, as done in the "MER zandwinning" project. Mussels and *Ensis* are represented as whole populations, assuming their size distributions remain constant.

3D-DCSM FM including water quality processes does not include fine sediment modelling at this stage. To account for the effect of inorganic suspended sediments on light climate, we use the weekly top-layer sediment field from the "MER zandwinning" project (representative of the year 2007). For more details on hydrodynamic and water quality model forcings (e.g., offshore boundaries, river inputs and atmospheric fields), please refer to the full model description from the WOZEP report (Zijl et al. 2021).

2.3 Simulation of seaweed dynamics (*Saccharina latissima*)

The nutrient uptake and growth dynamics of *S. latissima* are modelled with an updated version of the MALG module, developed within the IMPAQT project (Schueder and van Duren 2019).

MALG formulations are based on the model described from Broch and Slagstad (2012), representing macroalgae uptake of carbon and nitrogen as well as growth dynamics. On top of this, MALG also simulates the uptake and assimilation of phosphorus, using similar equations as for nitrogen. Additionally, MALG calculates the 3D vertical structure of the seaweed in 3D models (i.e. growth of the seaweed fronds throughout several vertical water layers). Thereby, the module can simulate the vertical gradients of the effects of seaweed growth in the water column.
In MALG, seaweed is represented by four distinct state variables representing its structural mass (MALS) and its carbon, nitrogen and phosphorus internal reserves (MALC, MALN, MALP). Collectively these components represent the entire macroalgae frond. The relationships between these variables and the ambient environment are shown in Figure 2.3.

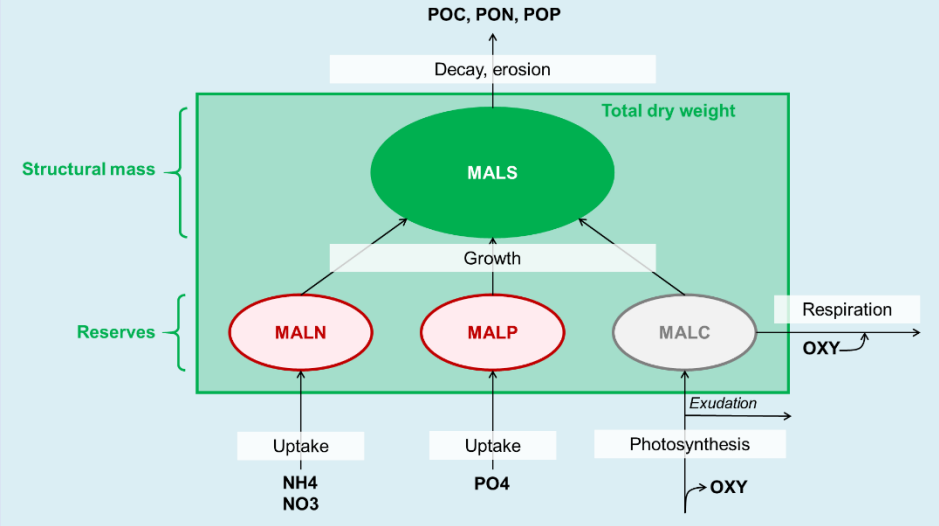

Figure 2.3: State variables and processes simulated with MALG module.

The structural mass (MALS) represents the part of the macroalgae that increases the area and length of the total frond when it grows. It grows by using carbon and nutrients from the frond's storage pools exclusively and produces detrital organic matter as it dies off/decays. MALS is assumed to have a fixed C:N:P composition and carbon to dry weight ratio. The ratio of stored mass to structural mass can however vary; the C:N and C:P ratios of the entire frond, and thus the dry matter, will therefore change in response to changes in the environment (Broch and Slagstad 2012).The nitrogen and phosphorus reserves (MALN and MALP) are constituted by the uptake of dissolved inorganic N (DIN = NH4+NO3) and P (PO4, referred to as DIP in the rest of the report) from the ambient water. Seaweed species have a maximum storage capacity for each of these nutrients. The carbon storage pool (MALC) is constituted by photosynthesis and provides carbon to the structural mass during growth periods. The relationship between volume and area of a seaweed frond is assumed constant. For a complete overview of equations and parameters used to describe seaweed dynamics, see Annex A (p. 40).

Table 2.2: Comparison of nutrient uptake parameters from Broch and Slagstad (2012; Norway) and Lubsch and Timmermans (2019; The Netherlands). Underlined values are those used in the model.

Parameter	Description	Value Broch and Slagstad (2012)	Value Lubsch and Timmermans (2019)
$\frac{MALN_{max}}{MALS}$	Maximum N reserves with respect to MALS (gN/gDW)	0.022	0.37 [a]
$J_{N,max}$	Maximum external DIN uptake rate (gN/dm^2/h)	1.4 10^{-4}	6.57 10^{-4} [b]
K_N	Half-saturation for external DIN uptake (µmol/L)	4	
$\frac{MALP_{max}}{MALS}$	Maximum P reserves with respect to MALS (gP/gDW)		0.14 [a]
$J_{P,max}$	Maximum external DIP uptake rate (gP/dm^2/h)		1.03 10^{-4} [b]
K_P	Half-saturation for external DIP uptake (µmol/L)		*1.5* [c]

[a] Measured internal storage capacity (per frond surface area), converted with dry weight to frond area ratio of 0.6 gDW/dm^2 from Broch and Slagstad (2012). This value is also consistent with measurements on *S. latissima* cultivated in the Dutch Oosterschelde (mean ratio of 0.64 gDW/dm^2 between March and May, personal communication Henrice Jansen).

[b] Measured surge uptake rate.

[c] Half saturation parameter was not estimated by Lubsch and Timmermans (2019). However, maximum uptake was observed for a nominal DIP concentration of 3.0 µmol/L.

Most parameters used in the present study are directly taken from Broch and Slagstad (2012, Table 2.2). However, in the latter study, the model is set up to simulate *S. latissima* in a fjord off the West coast of Norway, where environmental conditions are quite different from those off the Dutch coast. Most of all, the Dutch coast receives high nutrient inputs from rivers and is more open, leading to higher currents. This means that a seaweed farm off the Dutch coast will be subject to a higher nutrient throughflow than a farm with the same set-up in Norway. *S. latissima* cultivated off the Dutch coast is therefore most likely adapted to more nutrient-rich environments. We therefore use the recent results from Lubsch and Timmermans (2019) to parameterize nutrient uptake (Table 2.2).

2.4 Representation of seaweed farming areas in scenario runs

In all scenarios, the seaweed is assumed to grow on horizontal ropes, from the water surface downwards. The initial biomass is calibrated, based on previous modelling tests, to achieve a target cultivation yield of ~1 kgDW/m^2 at the end of the cultivation cycle. To reach this final biomass in the study area, off the Dutch coast, each farm is initialized with 3.84 gDW/m^2 of MALS, 2.32 gC/m^2 of MALC, 0.0384 gN/m^2 of MALN and 0.00384 gP/m^2 of MALP.

All scenario runs are described in Table 2.3. The corresponding extents of farming areas are mapped in Figure 2.4 and Figure 2.5.
In scenario runs using the coarse grid, it is not possible to represent seaweed farming over small areas, since the grid cells have an area > 50 km^2. In these scenarios, we assume that seaweed cultivation is carried out homogeneously over 25% of the test areas. We therefore divide initial seaweed biomasses by a factor 4 to reach a target cultivation yield of ~250 g/m^2 over these large test areas. We place these “test areas” in designated offshore windfarm (OWF) areas, since the multi-use of marine space is an important pillars of the Dutch marine spatial planning.
With the fine grid 3D-DCSM FM, it is possible to simulate seaweed cultivation in small farms (down to the size of one grid cell, i.e. ~0.8 km^2). With this version of the model, we test the effect of small-scale cultivation at different locations (i.e. farms of similar sizes as current seaweed cultivation test sites). We also assess the effect farm size within one area.

Table 2.3: Description of scenario runs.

Scenario	Model grid	Description
S-CRef	Coarse	Reference: no seaweed cultivation
S-C1	Coarse	Seaweed cultivation in all designated OWF areas (over 25% of surface)
S-C2	Coarse	Seaweed cultivation in ~100 km^2 patches in all major Dutch designated windfarm areas (over 25% of surface)
S-C3	Coarse	Seaweed cultivation in one ~100 km^2 patch in the Borssele OWF area (over 25% of surface)
S-FRef	Fine	Reference: no seaweed cultivation
S-F1	Fine	Seaweed cultivation in 1-cell farms in Borssele, ten noorden van de Waddeneilanden (TNWE), the North Sea Farm (NSF) and in the Voordelta
S-F2	Fine	Seaweed cultivation in one large farm covering 25% of the Borssele OWF area
S-F3	Fine	Seaweed cultivation in 107 1-cell farms covering 25% of the Borssele OWF area

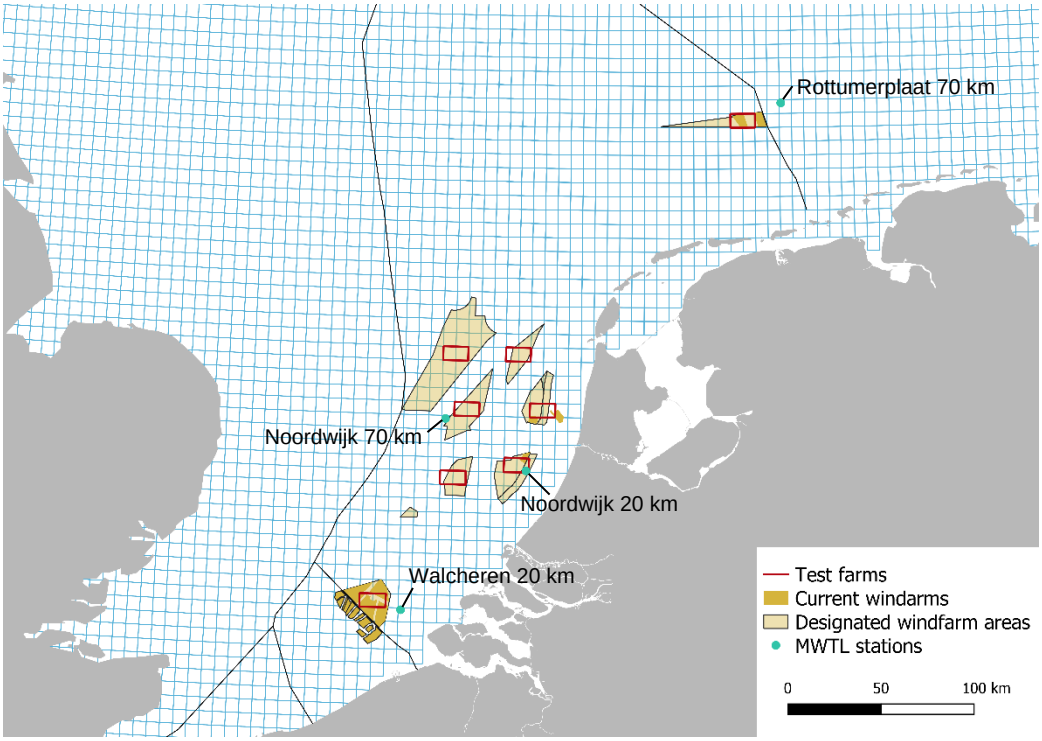

Figure 2.4: Coarse model grid, location of the designated OWF areas[1] and 2-cell farms (red squares) in scenario S-C2. MWTL stations used for model-observation comparisons are indicated with green dots.

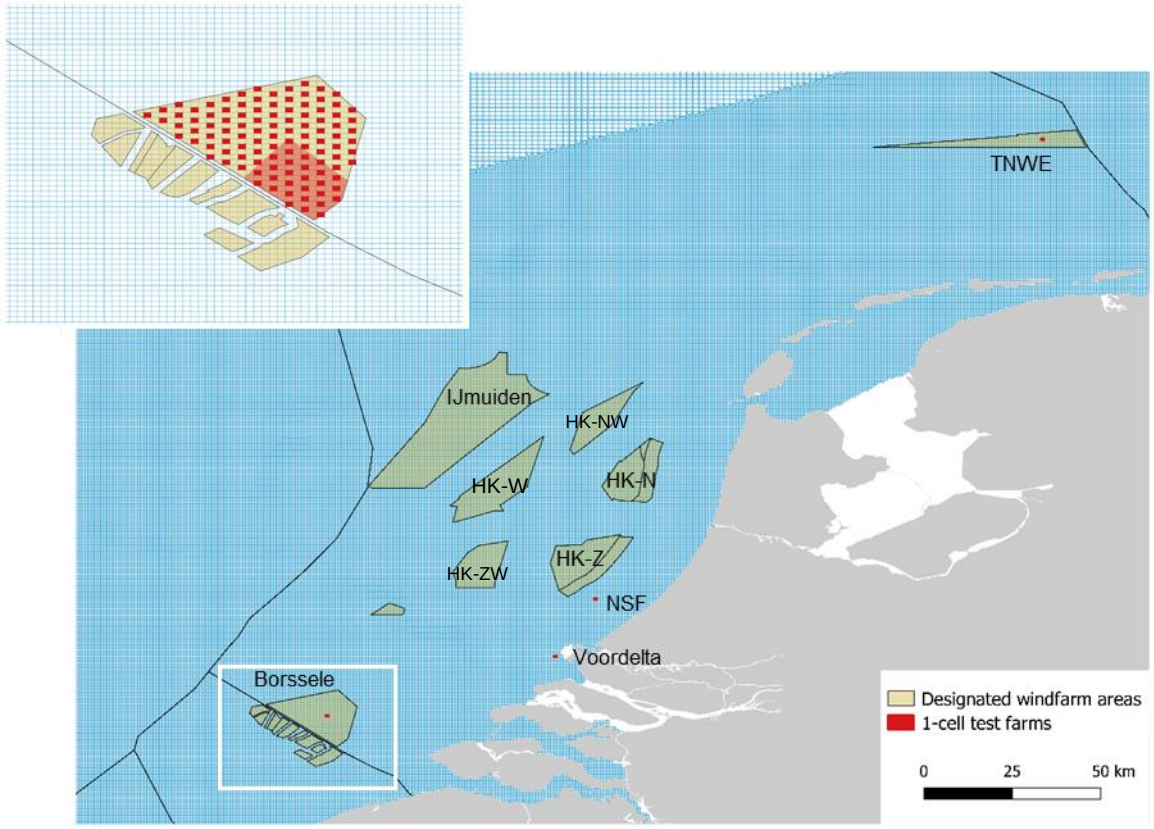

Figure 2.5: Fine model grid, location of the designated OWF areas[1] and 1-cell farms (red dots) in scenario S-F1. The zoomed-in map shows the extent of the one large farm of scenario S-F2 and the 107 1-cell farms of scenario S-F3, both covering ~25% of the total Borssele windfarm area.

[1] The locations of the "designated" OWFs we used are based on older delineations. Some of these have or are in the process of being changed (e.g. the IJmuiden-Ver area will likely be reduced and / or shifted northwards). In this study, we therefore worked with ***hypothetical scenarios***, meant to gain insight in ecosystem effects, not to provide actual realistic future impacts.

The model is run for one year, over a production cycle, from September 2016 to September 2017. It is initialized using 8 months of spin-up (January-August 2016). To avoid long spin-up times, the spin-up run is initialized using 3D fields from the Copernicus Marine Service global ocean biogeochemistry hindcast for active constituents, and 2D fields from the “MER zandwinning” model for non-transported variables (bottom detritus, mussels and *Ensis*).
All processes are calculated at a 10 min time step, except for those related to the BLOOM module that has a daily time step. Time-series outputs are produced at a daily timestep at several locations (seaweed farm locations and four MWTL stations) and map outputs are printed at a weekly interval. On top of this, mass balance outputs are produced to help with the system understanding.
Maps presented in this report show average values over the winter (December-February) or the spring period (March-May). To visualize the effects of seaweed cultivation for the different simulated scenarios, we also plot maps of the percentage difference of winter nutrient surface concentrations and of spring phytoplankton primary production. Differences in phytoplankton primary production are examined over spring, since it corresponds to the period of highest phytoplankton growth (covering the spring bloom). Winter mean inorganic nutrients can explain a large part of observed spatial variability in growing season mean chlorophyll-a concentrations (Blauw et al. 2019). We therefore map the differences in these winter concentrations between scenario and reference runs, as a proxy to explain changes in spring phytoplankton primary production.
For the different simulated scenarios, we define as “footprint area” of a seaweed farm, or of an ensemble of farms, for a certain variable (DIN or DIP winter surface concentration, spring phytoplankton primary production), the area over which the value of this variable differs by more than 1% with respect to the reference run.

Maps of absolute differences in spring DIN and DIP surface concentrations and phytoplankton primary production can be found in Appendix B (p. 43).

3 Model results

3.1 Model validation

According to the validation carried out within the WOZEP project for the year 2007 (Zijl, 2021), the model is very reliable to simulate water flows and stratification and reproduces the overall temporal patterns of major nutrients, chlorophyll-a and oxygen at MWTL monitoring locations rather well. However, the coupled hydrodynamic-water quality model is still in its development phase, and some discrepancies with measurements were noted. It seems that the model simulates a too early increase in DIN concentrations at the end of the summer at the most Southern monitoring locations (e.g., Noordwijk), which could be caused by an underestimation of nitrogen retention in bottom sediments. Moreover, the model overestimates spring P depletion at all MWTL stations, while NO3 depletion is underestimated in some locations. The simulated phytoplankton biomass being very consistent with measurements, and winter nutrient levels well reproduced by the model, it seems that the N:P ratio of nutrient uptake by phytoplankton may be underestimated.
The coarse-grid model provides very similar results to the fine-grid model for all water quality variables, except for locations close to complex shorelines (e.g., near Terschelling island). We therefore concluded that the coarse-grid model is an adapted tool to test new model developments and get first estimates of the effects of seaweed cultivation at offshore locations.

We compare here simulated time series of NO3, PO4, chlorophyll a and oxygen to measurements at four MWTL monitoring stations for the study period (September 2016 to September 2017). These four stations were picked due to their proximity to designated OWF areas (Figure 2.4). The conclusions of this model-observation comparison are similar to those for the year 2007. The model reproduces winter concentrations of dissolved inorganic nutrients at all stations well (Figure 3.1). As for 2007, the model simulates an increase in inorganic nutrient concentrations from mid-summer to winter, while the measurements show that this increase usually starts only in late fall/winter. The model simulates PO4 depletion at all four monitoring locations during the summer, while low concentrations are measured. At Walcheren 20 km and Noordwijk 20 km, nitrogen depletion is underestimated.
Chlorophyll a levels and the temporal dynamics thereof are well reproduced by the model. Only the very high value measured at Walcheren 20 km in spring 2017 was not captured.
The drop in oxygen concentrations at the Noordwijk stations in winter is not reproduced. This drop seems to coincide with a rapid increase in NO3 concentrations, which could indicate that there has been a rapid re-mineralization of organic matter, which occurred slower and over the entire fall period in the model.

At this stage, no data is available to validate the simulated seaweed dynamics in the environment.

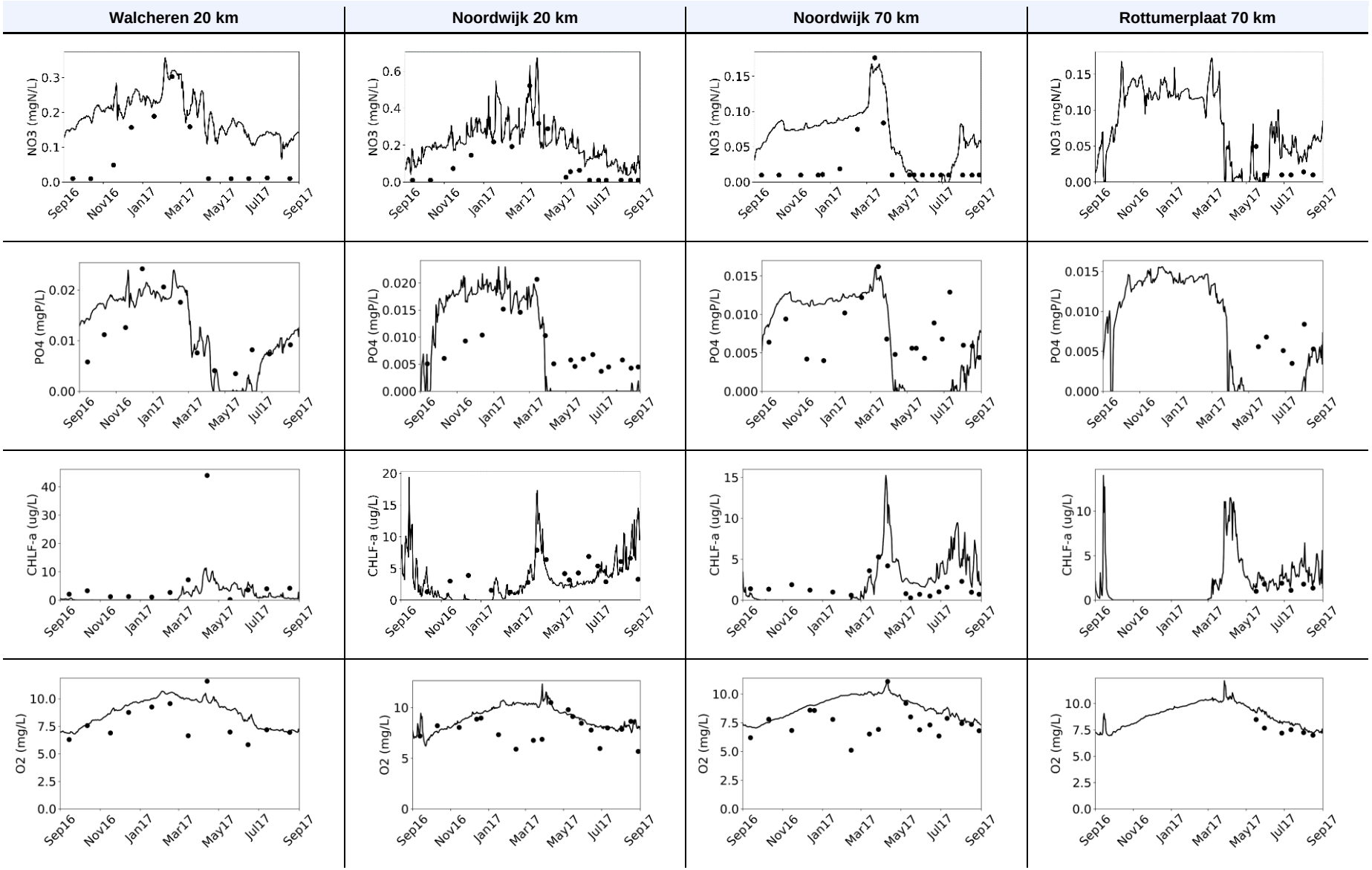

Figure 3.1: Comparison of simulated and measured time series of NO3, PO4, chlorophyll a and oxygen at four MWTL stations for the study period.

3.2 “Reference” nutrient concentrations and phytoplankton primary production

Average winter DIN surface concentrations are quite spatially homogeneous, around 0.1-0.2 mgN/L, far off the Dutch shore (Figure 3.2 – top-left). Within a ~30-35 km strip, concentrations gradually increase towards the coast. Surface DIN concentrations are generally close to 0.3 mgN/L near the coast and up to 1 mgN/L in estuaries. In spring, offshore surface DIN is nearly depleted (Figure 3.2 – top-right). However, nearshore concentrations remain similar to the winter ones, up to 30-35 km from the coast.

Spatial gradients of surface DIP concentrations are generally less steep than those of DIN. Winter DIP concentrations reach ~0.015 mgP/L offshore from the Dutch coast (Figure 3.2 – bottom-left). The concentrations slightly increase towards the coast to 0.02-0.025 mgP/L, and up to 0.03-0.04 mgP/L in estuarine areas. In spring, there is generally less DIP depletion than for DIN in offshore areas. Offshore, spring surface DIP concentrations are mostly still >0.005 mg/L (Figure 3.2 – bottom-right). Contrary to DIN, zones of extremely low DIP concentrations occur nearshore, off the Belgian coast and South of the Wadden islands. In other coastal areas, the increase in concentrations linked to river outflows is limited, both in terms of intensity and in area of influence (up to ~15 km from the river outlet).

Average spring phytoplankton primary production reaches values of 0.5-1.5 gC/m^2/day in the North Sea off the Dutch coast (Figure 3.3). It is lower in the Wadden Sea, where spring DIP may be limiting and higher suspended sediment concentrations limit light availability. Directly North-East of the English Channel and in the area of influence of the Scheldt river, phytoplankton primary production is near-zero due to high turbidity (i.e. light limitation).

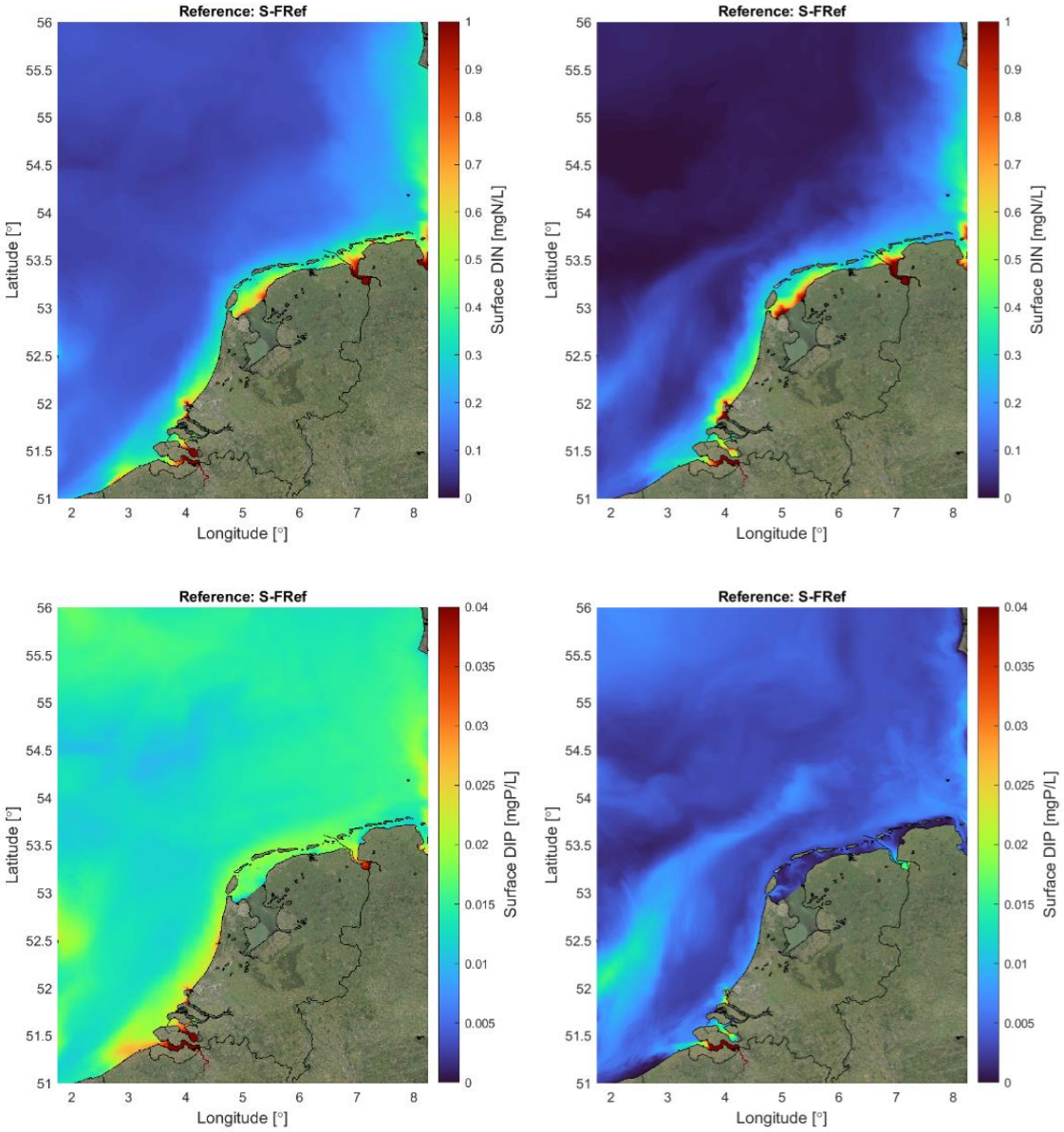

Figure 3.2: Simulated mean surface inorganic nutrient concentrations. Top: DIN. Bottom: DIP. Left: winter (December-February). Right: spring (March-May).

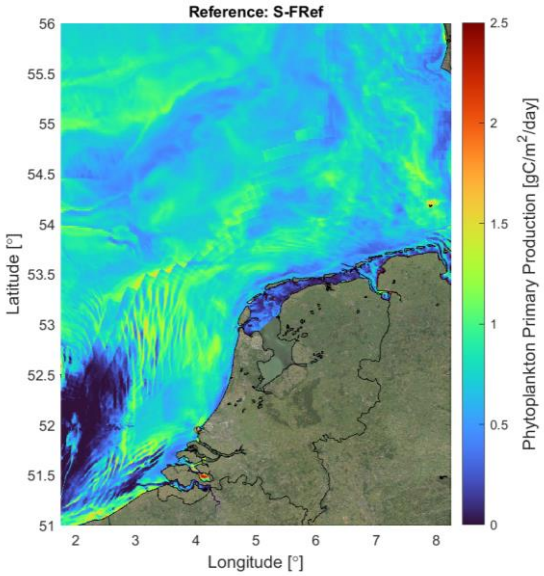

Figure 3.3: Simulated mean spring phytoplankton primary production per surface area.

3.3 Seaweed production

With the current model set-up and formulations for seaweed dynamics, seaweed cultivation does not seem to hit any limitation for the target yields and farm extents of the different scenarios (i.e. target yield is always reached at the end of the simulation).

In the model, carbon reserves constitute most of the dry weight of the total seaweed biomass (Figure 3.4A). Around the harvesting period (June), structural biomass constitutes the second largest pool. If seaweed is left to grow further in the summer, the fronds start to slowly die off due to temperature and light conditions. External nutrients are limiting for the constitution of internal reserves from April to July (Figure 3.4B)
However, the nutrient reserves constituted during the winter period are sufficient to sustain the growth until June (Figure 3.4C and D)
.

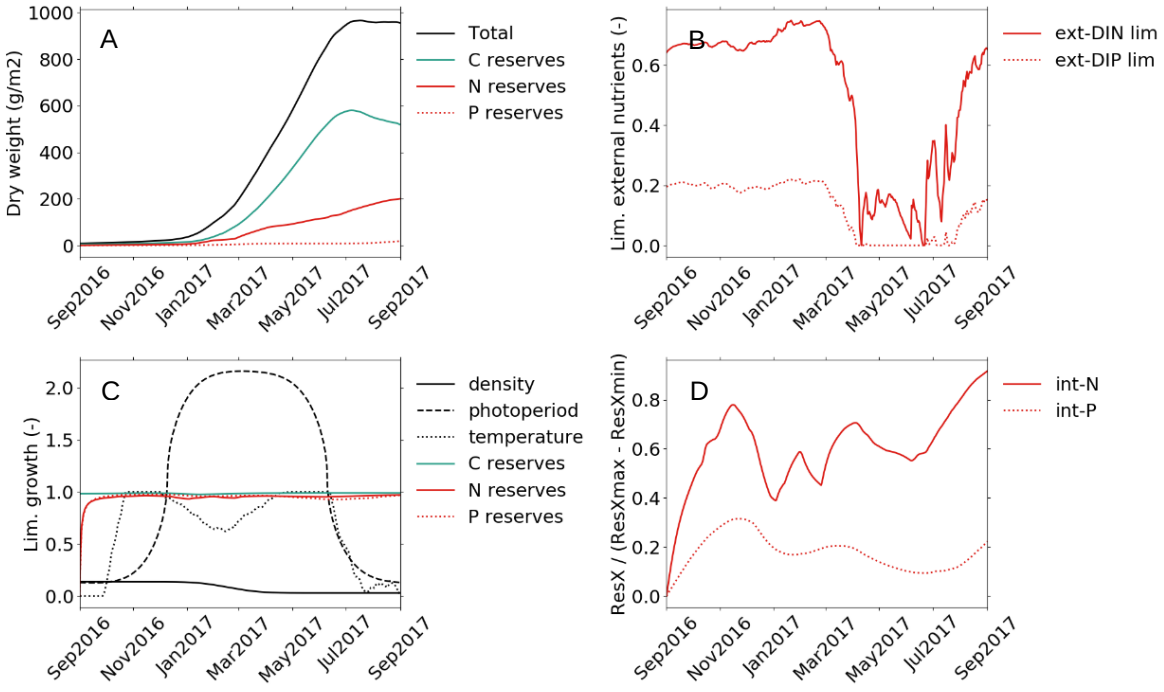

Figure 3.4: Seaweed dynamics in Borssele farm in scenario S-C2. A: Dry weight of the different seaweed constituents. B: Limitation factors for the uptake of external nutrients (growth of reserves). C: Limitation

factors for the growth of structural biomass. D: Proportion of storage capacity filled (ResX=amount of stored nutrient X, ResXmax – ResXmin=total storage capacity).

Seaweed dynamics have a significant effect on the carbon and nutrient cycles in the farming areas (Figure 3.5). Seaweed primary production and nutrient uptake rates are of the same order of magnitude as those of phytoplankton. However, their temporal patterns differ. Nutrient uptake and carbon storage by seaweed starts early in winter.

At Borssele, where the nitrogen throughflow is not limiting in spring, but phosphorus concentrations become extremely low, the seaweed continues to store nitrogen throughout the growing season but grows almost exclusively on its internal phosphorus reserves.

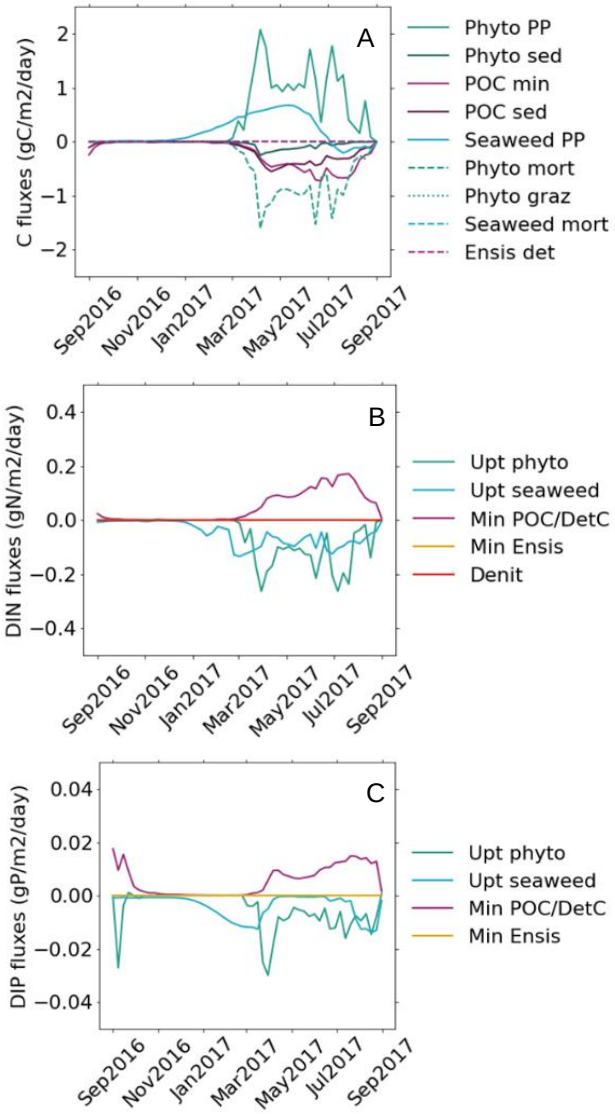

Figure 3.5: Process rates in Borssele farm in scenario S-C2. A: Organic C fluxes. B: DIN fluxes. C: DIP fluxes.

3.4 Maximum upscaling scenario of seaweed production

3.4.1 Winter nutrient concentrations

Upscaling of seaweed cultivation over 25% of all designated OWF areas leads to a clear decrease in winter (December-February) nutrient concentrations along the entire Dutch coast (Figure 3.6). The maximum effect occurs close to/in the IJmuiden-Ver windfarm area, where DIN surface concentrations with seaweed cultivation are ~20% lower than in the reference run and DIP surface concentrations ~15% lower. The fact that the largest effect is near IJmuiden-Ver is probably due to the size of that windfarm area (> 1/3 of the surface of all designated areas), combined with the fact that this windfarm is located quite far offshore, away from the influence of high nutrient freshwater input. An exacerbating effect may result from interactions between farm areas. This zone of maximum nutrient reduction is “downstream” from other OWFs such as Borssele, so nutrient concentrations of the inflowing water are already impacted by seaweed farming earlier along the flow path. Such a set-up leads to a >10% decrease of DIN concentrations over an area of 1944 km^2 and of DIP over an area of 1546 km^2. Even though the effect on DIN is more intense (in terms of relative decrease in concentrations), the DIP footprint has a larger spatial extent: decreases of DIP greater than 1% occur over an area greater than 40,000 km^2, which is 1.5 times greater than the area with a >1% DIN decrease.

This is due to the fact that DIP concentrations are more homogeneous over space, with a less steep increase along the coast. Indeed, a decrease in DIN concentrations off the Danish coast and in the Wadden Sea, where concentrations are higher, has a smaller relative effect than offshore, while for DIP concentrations in these areas are similar to those offshore.

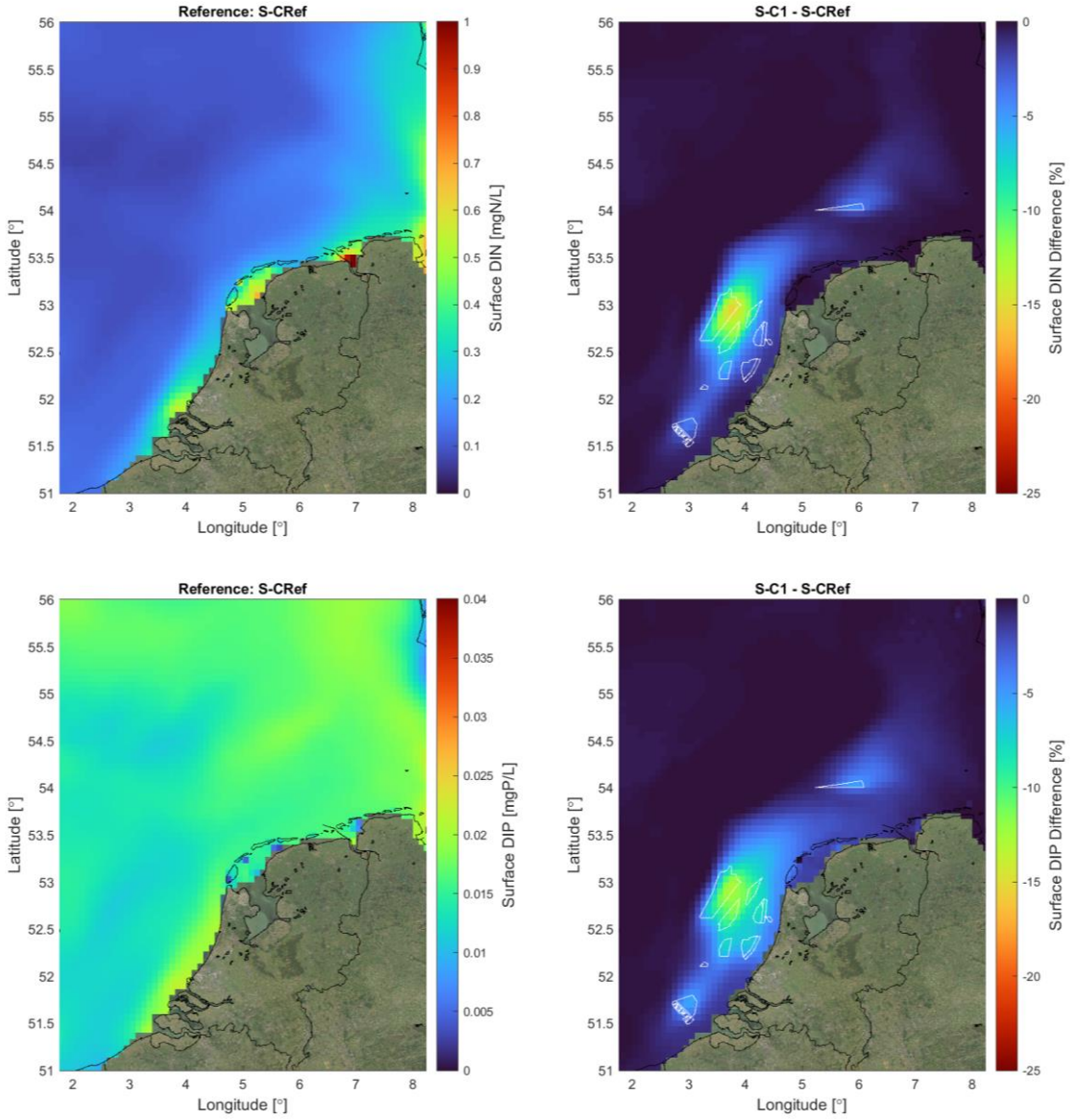

Figure 3.6: Effect of seaweed cultivation over 25% of all designated OWF areas (scenario S-C1) on winter nutrient concentrations. Top: surface DIN. Bottom: surface DIP. Left: concentrations in reference simulation. Right: difference between scenario run and reference in %.

3.4.2 Spring phytoplankton primary production

In spring (March-May), the decrease in ambient nutrient concentrations has a strong effect on phytoplankton primary production, that drops along the entire Dutch coast. A maximum drop of ~30% is simulated in the South-Eastern corner of the IJmuiden-Ver windfarm area (Figure 3.7). This area corresponds with the area where winter surface inorganic nutrient concentrations are the most affected by seaweed cultivation as well. A decrease in phytoplankton primary production of ~25% is also simulated east from the TNWE OWF area. This area coincides with the area of highest absolute decrease in spring surface DIP concentration (of ~0.0015 mgP/L) (Figure B.1). A decrease in spring phytoplankton primary production of more than 10% occurs over an area greater than 20,000 km^2. The footprint area in terms of spring phytoplankton primary production (reduction >1%) of such a large-scale cultivation set-up covers 57,312 km^2.

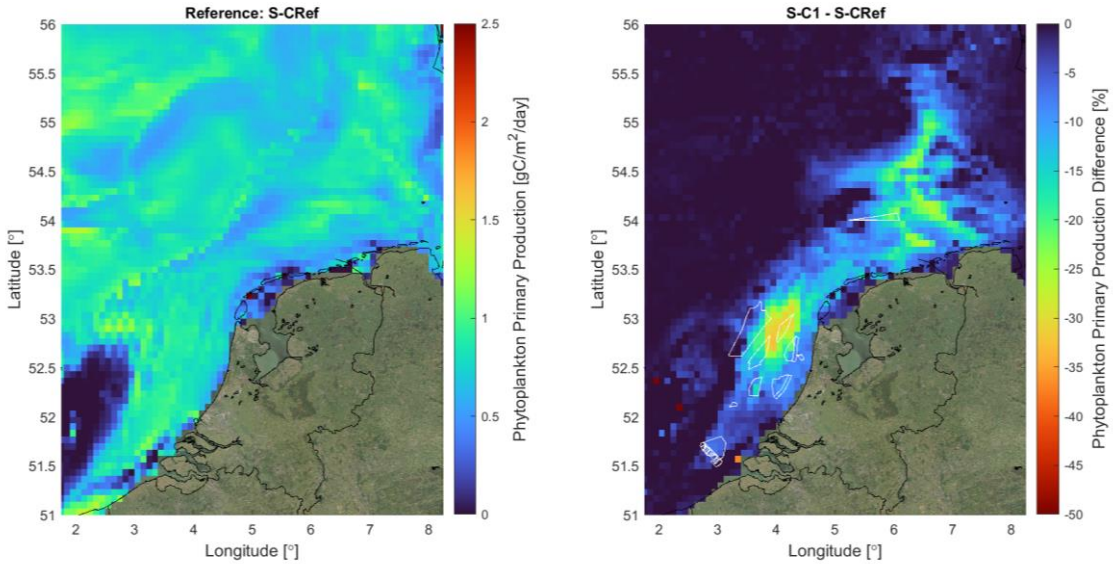

Figure 3.7: Effect of seaweed cultivation over 25% of all designated OWF areas (scenario S-C1) on spring phytoplankton primary production. Left: concentrations in reference simulation. Right: difference between scenario run and reference in %.

3.5 Seaweed production in farms of equal size (~100 km^2)

3.5.1 Cultivation within all designated OWF areas

When getting rid of the size effect, i.e. when simulating farming areas of equal size at the different OWF locations, the strongest effect on winter nutrient reduction and spring phytoplankton primary production (in %) is indeed not simulated in the IJmuiden area, but closer to the shore, and further North East (Figure 3.8). In scenario S-C2, the cultivation area is reduced by a factor 4 compared to scenario S-C1 (~200 km^2 against 790). At this scale the effect of seaweed farming on nutrient and phytoplankton production is still significant. Winter surface DIN and DIP concentrations are reduced by >1% over areas of 7,061 km^2 and 11,803 km^2, respectively, and reach more than 3%.Spring phytoplankton primary production drops up to ~10% around the OWF area Hollandse Kust Noord-West (noted HK-NW, see map in Figure 2.5 for location). Reduction in spring phytoplankton primary production >1% occurs over an area of 37,575 km^2.

The reduction in nutrient concentrations linked to one farm extends outside of the cultivation areas in the direction of the current, which leads to interaction effects between the farm areas. The North-Eastern farms receive lower nutrient inputs due to uptake in South-Western farms, adding up to the effect of the local seaweed cultivation. To better grasp this interaction effect, we calculated the annual phytoplankton primary production in OWF area HK-NW, where effects in scenario S-C2 are the largest, for 3 situations (Table 3.1): 1) without cultivation, 2) with cultivation in ~100 km^2 plots in all OWF areas and 3) with cultivation only in the OWF HK-NW plot. The results show that, while cultivation over 25% of a ~100 km^2 plot in OWF HK-NW only leads to a decrease in annual phytoplankton primary production of 3 gC/m^2 (1.4%), phytoplankton primary production is reduced by 8 gC/m^2 (3.7%) locally when seaweed is cultivated in other OWFs as well.

Table 3.1: Simulated annual primary production at OWF area HK-NW (see Figure 2.5 for location) in reference run, with farms of equal size in all OWFs and with the farm in OWF HK-NW only.

Simulation set-up	Annual phytoplankton production within OWF HK-NW (gC/m^2)
Reference: S-CRef	214
Cultivation over ~100 km^2 all OWF areas: S-CF2	206
Cultivation over ~100 km^2 of OWF HK-NW	211

3.5.2 Cultivation in Borssele windfarm area

Seaweed farming at a single location (over 25% of a ~100 km^2 patch in Borssele windfarm area only – scenario S-C3), the local maximum reduction in winter surface DIN and DIP concentrations are 0.75% and 1.6%, respectively (Figure 3.9). A decrease in DIP concentrations >1% with respect to the scenario without seaweed occurs over an area of 512 km^2. The maximum drop in spring phytoplankton primary production linked to this single farm is <2%, when cultivating *S. latissima* over 25 km^2 in the Borssele windfarm area at a yield of ~1 $kgDW/m^2$ over a production cycle. However, phytoplankton primary production is reduced by more than 1% over an area of 3,060 km^2 (300 times larger than the cultivation area), which extends North-East from the farm, in the direction of the current, up to the area North of the Wadden islands.

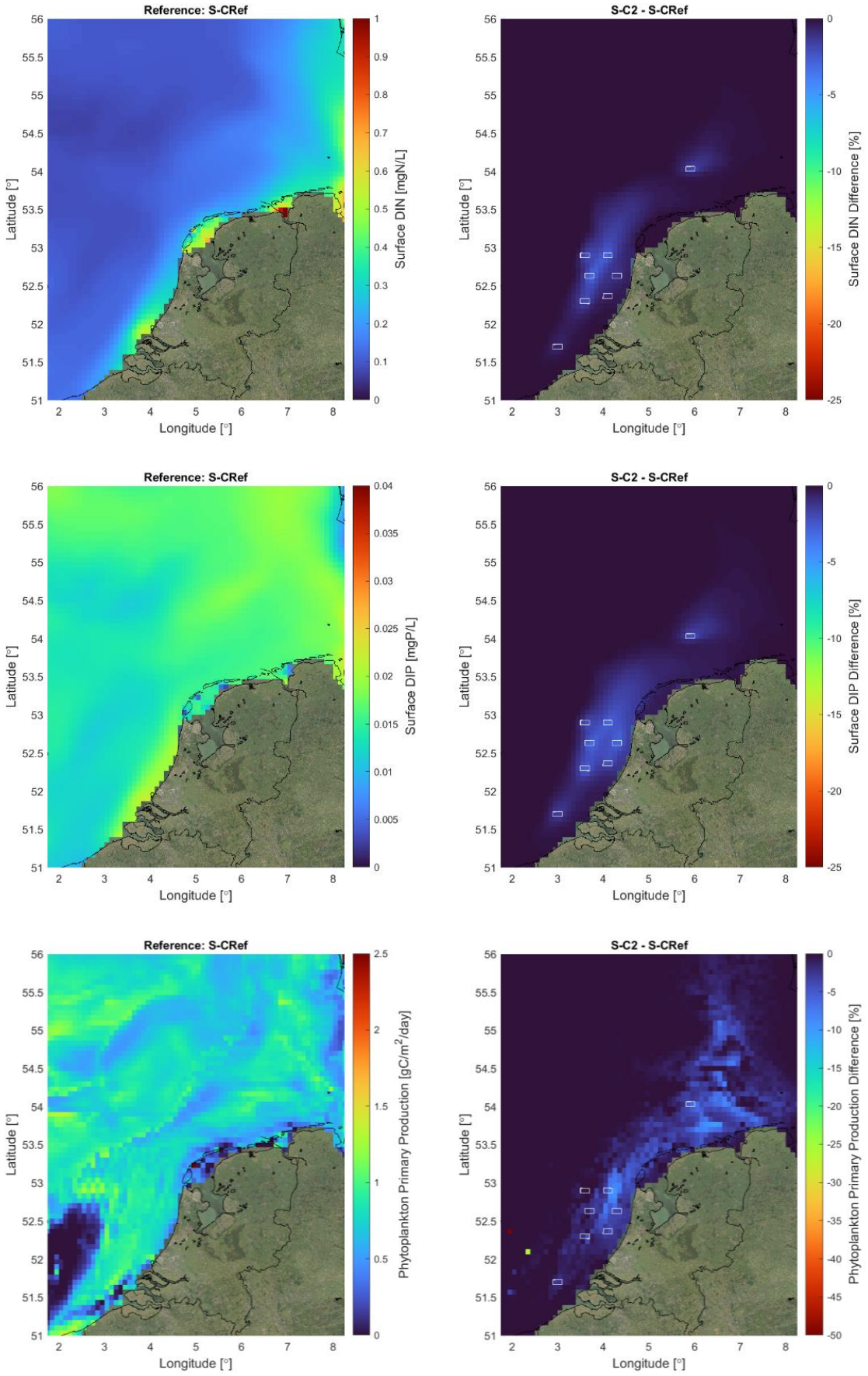

Figure 3.8: Effect of seaweed cultivation over 25% of ~100 km^2 patches in OWF areas (scenario S-C2) on winter nutrient concentrations and spring phytoplankton primary production. Top: surface DIN. Middle: surface DIP. Bottom: Phytoplankton primary production. Left: concentrations in reference simulation. Right: difference between scenario run and reference in %.

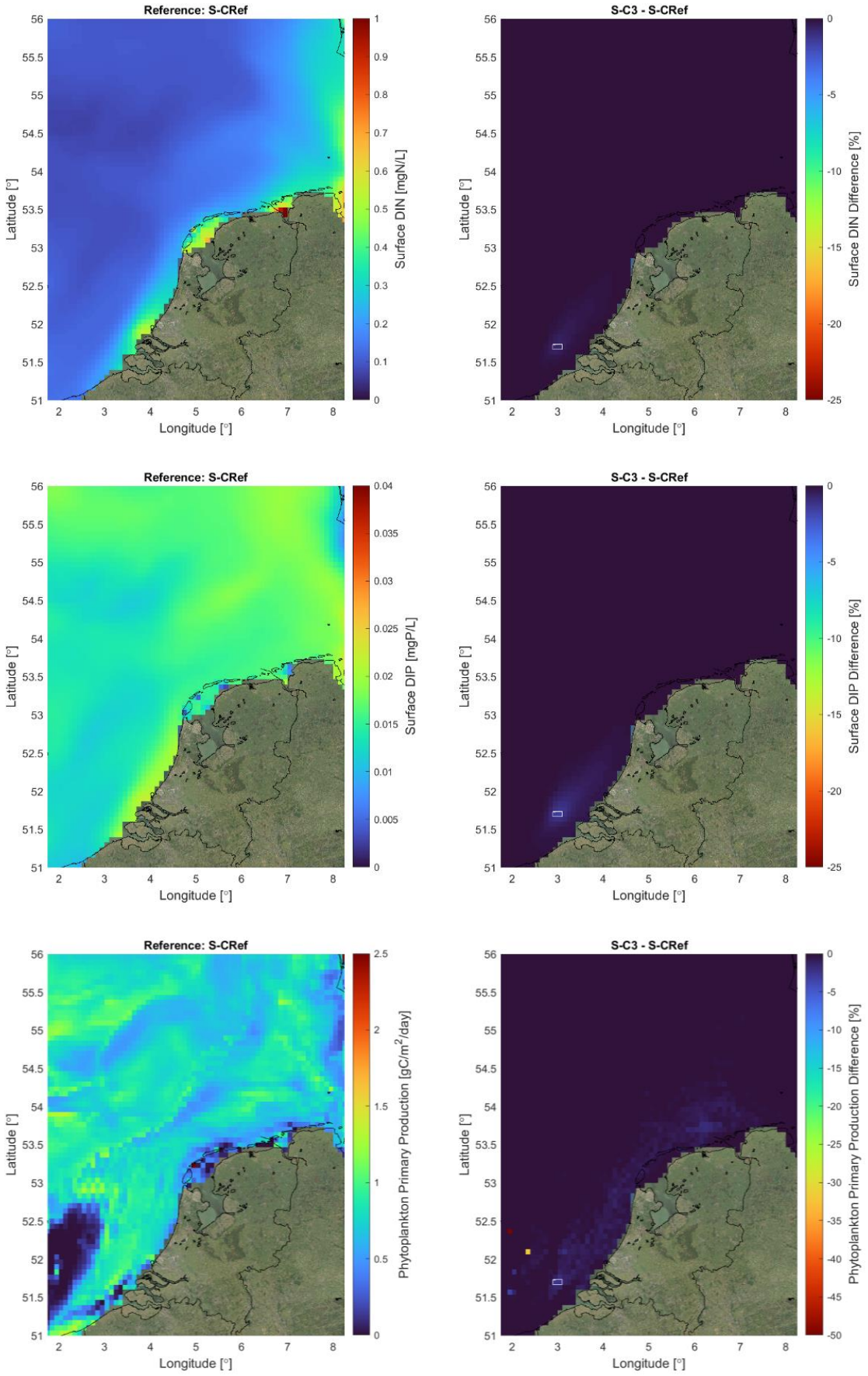

Figure 3.9: Effect of seaweed cultivation over 25% of a ~100 km^2 patch in the Borssele windfarm area (scenario S-C3) on winter nutrient concentrations and spring phytoplankton primary production. Top: surface DIN. Middle: surface DIP. Bottom: Phytoplankton primary production. Left: concentrations in reference simulation. Right: difference between scenario run and reference in %.

3.6 Effect of small-scale seaweed production at different locations

In scenario S-F1, we tested the effect of seaweed production in farms of ~0.8 km^2 at four different locations: Borssele, at the North Sea Farm (NSF), in the Voordelta and in the TNWE OWF designated area. This corresponds to a production scale currently already tested in the field.

Borssele and TNWE designated OWF areas seem to be more productive seaweed cultivation locations than the North Sea Farm and Voordelta areas (Table 3.2). This can most likely be related to the higher currents in these areas, generating more nutrient throughflow, and lower phytoplankton primary production, i.e. lower competition for external nutrients in the last months of the growing season.

At this scale of cultivation, the local effect on phytoplankton primary production is limited (< 1% at all four locations), both in terms of annual mean and spring values. The uptake of dissolved inorganic nutrients by seaweed within the four simulated farming locations has very little effect on DIN and DIP concentration dynamics over the production year (Figure 3.10 and Figure 3.11). Spatial variations in the effects on winter DIN and DIP surface concentrations and spring phytoplankton primary production are mapped in Figure 3.12 (note that the range covered by the color scale for relative differences with reference run is 10 times smaller than in other Figures).

Table 3.2: Amount of seaweed produced, annual phytoplankton primary production without seaweed and relative decrease with seaweed at the four cultivation locations in scenario S-F1.

	Borssele	**NSF**	**Voordelta**	**TNWE**
Seaweed production (gDW/m^2)	978	870	759	970
Annual phytoplankton production in reference run (gC/m^2)	202	269	255	188
Reduction in annual phytoplankton production (%)	0.07	0.35	0.48	0.67
Reduction in spring phytoplankton production (%)	0.06	0.58	0.65	0.62

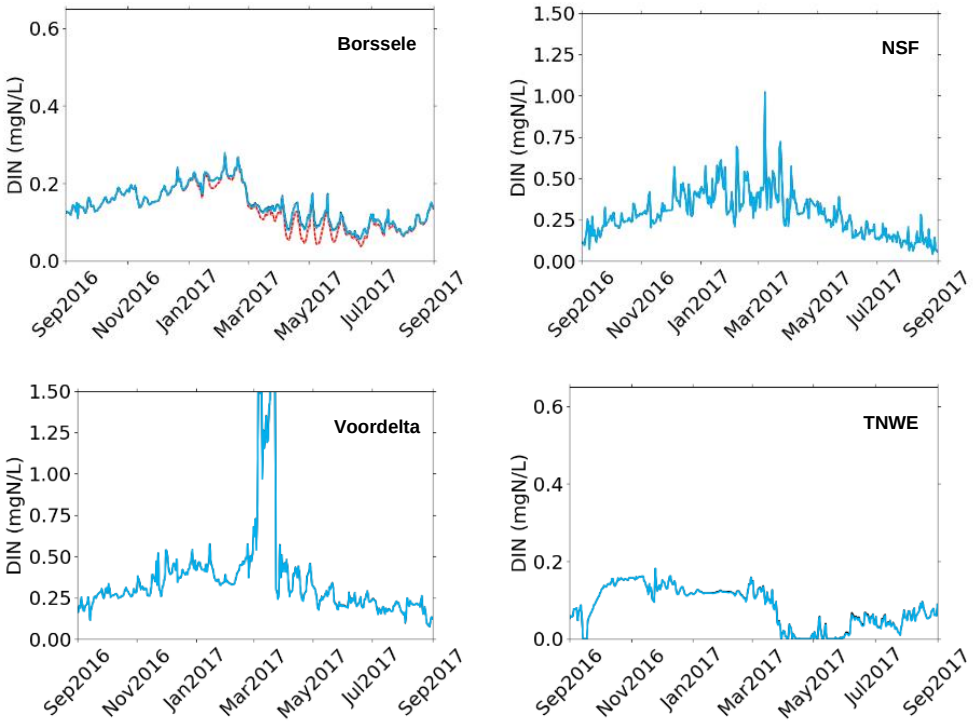

Figure 3.10: Simulated DIN concentrations at the four seaweed cultivation locations in S-F1. Black line=reference (S-FRef), blue line=with small-scale seaweed production (S-F1), red line=with seaweed production in one large farm covering 25% of Borssele OWF area (S-F2), pink dotted line=with seaweed production in 107 small farms covering 25% of Borssele OWF area (S-F3). Note that y-axis ranges differ.

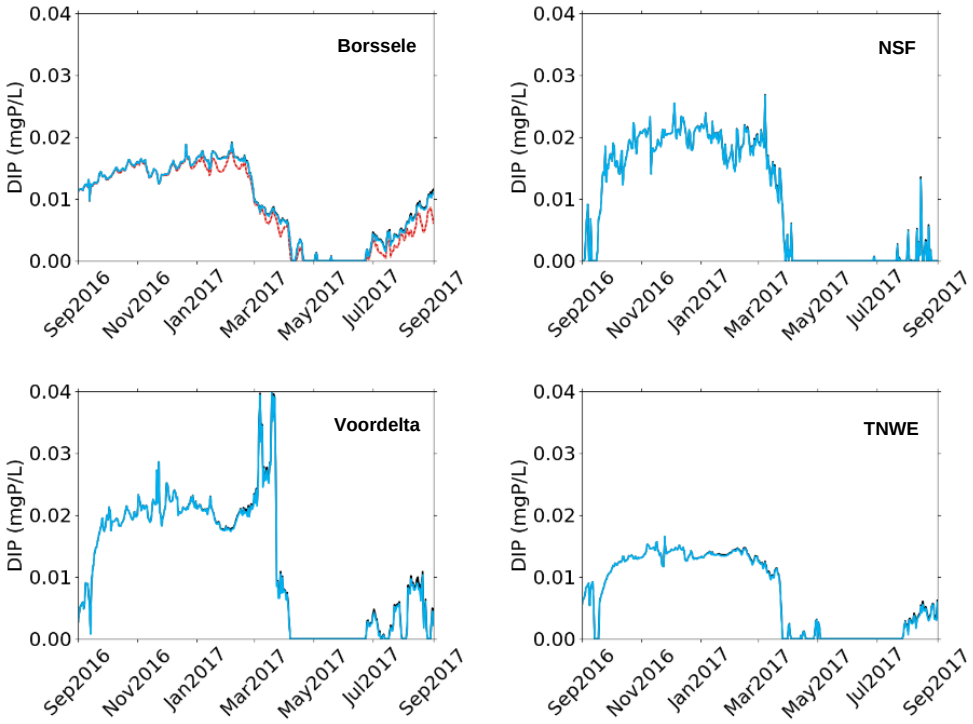

Figure 3.11: Simulated DIP concentrations at the four seaweed cultivation locations in S-F1. Black line=reference (S-FRef), blue line=with small-scale seaweed production (S-F1), red line=with seaweed production in one large farm covering 25% of Borssele OWF area (S-F2), pink dotted line=with seaweed production in 107 small farms covering 25% of Borssele OWF area (S-F3).

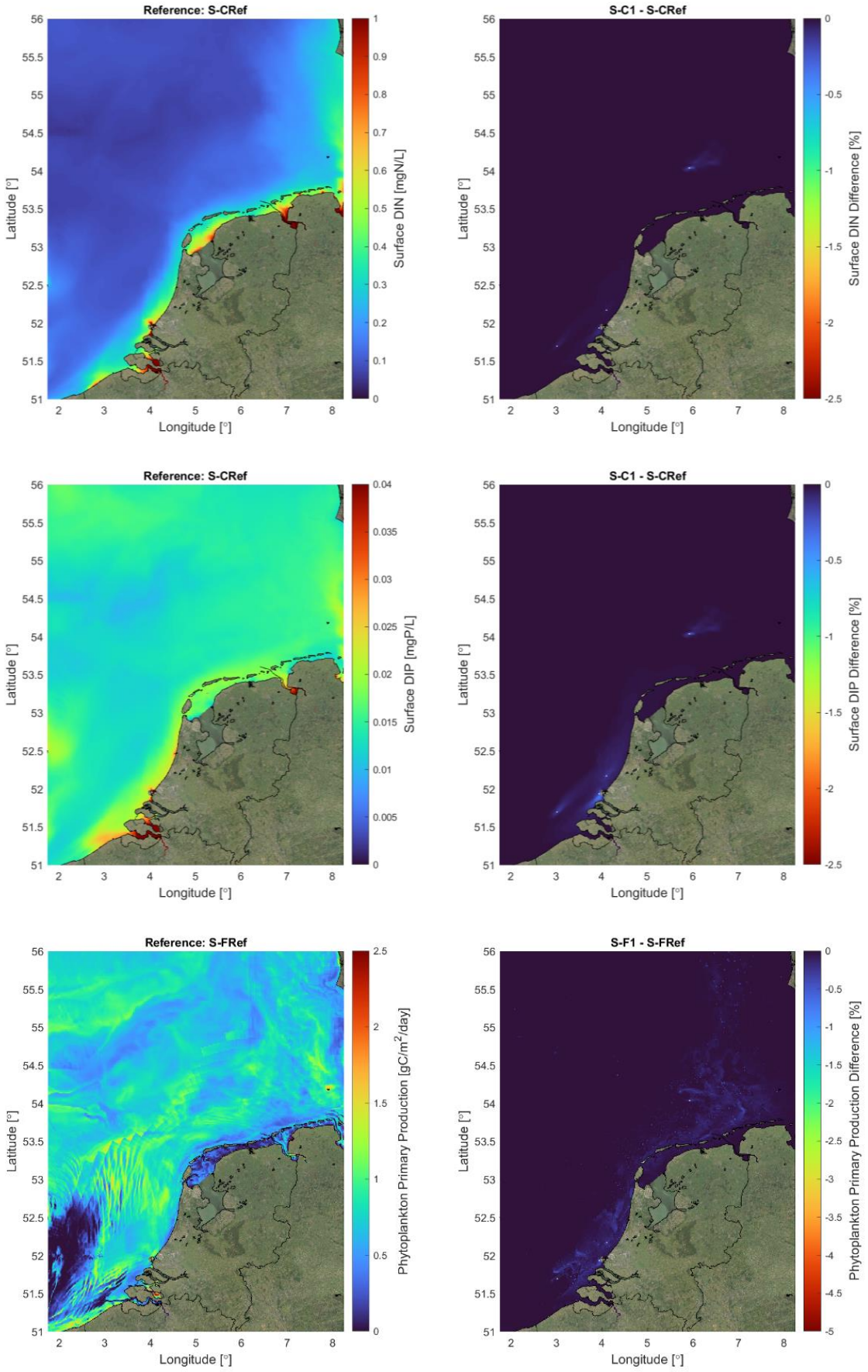

Figure 3.12: Effect of seaweed cultivation 1-cell farms (~0.8 km^2) in Borssele, the NSF, Voordelta and TNWE (scenario S-F1) on spring phytoplankton primary production. Left: concentrations in reference simulation. Right: difference between scenario run and reference in %.

3.7 Tests on spatial cultivation layouts at Borssele

On top of tests on the effect of size and location of seaweed cultivation areas, we tested the effect of different cultivation layouts within one large OWF designated area, Borssele. We assume that seaweed is cultivated over 25% of the Borssele OWF area, which represents a surface area of ~87 km^2. In scenario S-F2, seaweed production is carried out in one single large farm. In scenario S-F3, it is carried out within 107 1-cell farms, homogeneously distributed over the entire Borssele OWF (Figure 2.5).

Seaweed production is slightly (+7%) more productive when the cultivation is spread throughout the entire OWF area (scenario S-F3, see Table 3.3).

The environment footprint in terms of winter nutrient concentrations and spring phytoplankton primary production of seaweed cultivation at such a large scale extends over a large spatial area (Figure 3.13, Table 3.3). Indeed, for both scenarios, winter DIN and DIP concentrations are reduced by >1% over areas of ~1,000-2,000 km^2 and ~5,000 km^2 respectively and spring phytoplankton primary production drops by more than 1% over an area of almost 20,000 km^2, extending along the entire Dutch coast. The effect on winter DIP concentrations in terms of % reduction compared to the reference scenario is larger than that on winter DIN, both in terms of maximum intensity and spatial extent. This is probably due to the fact that DIP is more limiting than DIN in that area, and DIP uptake by seaweed occurs almost exclusively over the winter period (Figure 3.4). The highest percentages of reduction of spring phytoplankton production do not occur within the Borssele OWF area, but slightly more North-East, in the direction of the residual current, where nutrient and phytoplankton biomass concentrations are higher due to large river inputs. Cultivation of seaweed within the Borssele OWF, over an area of 87 km^2, leads to a reduction in spring phytoplankton primary production of more than 5% over more than 2,500 km^2 (Table 3.3). It is difficult to distinguish, based on these results, which cultivation set-up has a smaller environmental footprint. However, the extent over which phytoplankton primary production is reduced by more than 10% is 1/3 smaller when the cultivation is spread over the entire OWF area (S-F3), compared to when it is concentrated in one large farming area.

Table 3.3: Seaweed production and extent of the environmental footprint in terms of relative reduction in dissolved inorganic nutrients and phytoplankton primary production in scenarios S-F2 and S-F3.

		One large farm (scenario S-F2)	**107 1-cell farms (scenario S-F3)**
Seaweed production (gDW/m^2)		918	983
Area of winter DIN reduction (km^2)	**>1%**	1,117	2,064
	>5%	0	0
	>10%	0	0
Area of winter DIP reduction (km^2)	**>1%**	5,864	5,255
	>5%	261	219
	>10%	0	0
Area of spring phytoplankton primary production reduction (km^2)	**>1%**	19,467	19,972
	>5%	2,561	2,713
	>10%	1,062	723

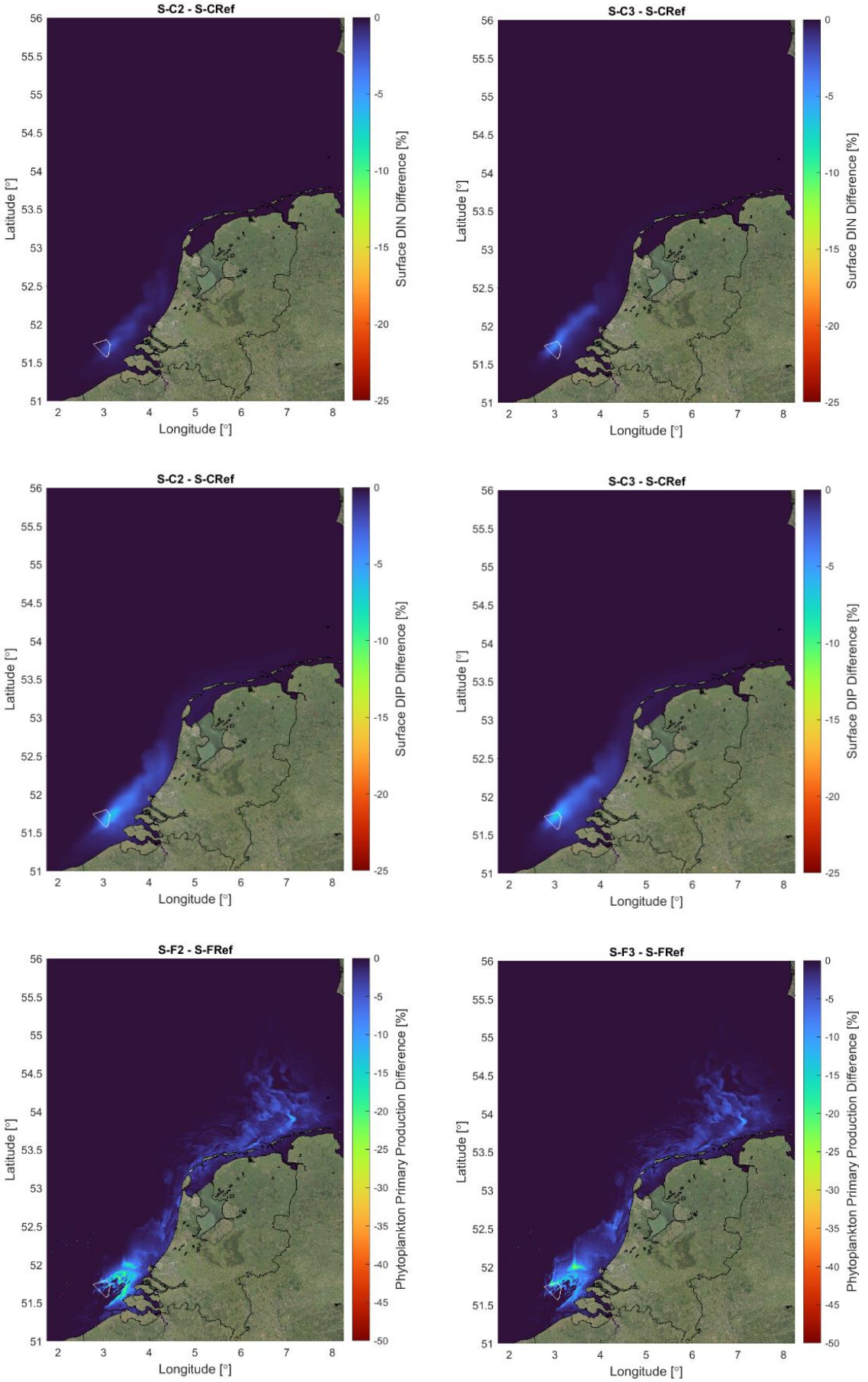

Figure 3.13: Effect of seaweed cultivation on winter nutrient concentrations and spring phytoplankton primary production for different farming set-ups at Borssele. Top: surface DIN. Middle: surface DIP. Bottom: Phytoplankton primary production. Left: difference between scenario run S-F2 (one large farm) and reference in %. Right: difference between scenario run S-F3 (107 1-cell farms) and reference in %.

4 Discussion and future steps

4.1 Effects of farm set-ups on seaweed production

According to the model results, and as already shown in the IMPAQT project (Vilmin and van Duren 2019), offshore areas (e.g., Borssele OWF area) seem to be slightly more suitable for seaweed cultivation than those closer to the coast, even though ambient nutrient concentrations are slightly lower. We relate this to the higher currents that lead to higher nutrient throughflow. Lower spring phytoplankton biomass also allows for the seaweed to continue nutrient uptake longer in the growing season. However, even though these systems can be slightly more productive, they will incur higher operational costs due to their distance to the coast.

The model results show that the growth of total seaweed biomass is mainly driven by temperature and light. For all tested scenarios and at all locations, seaweed production of 0.75 to 1 kgDW/m^2 could be reached. First tests on cultivation set-ups indicate that systems where farming is split into smaller plots are slightly more productive than when it is concentrated over one larger area (scenarios S-F2 and S-F3). In reality this difference may be even larger when effects of seaweed on local current velocities is taken into account, which is expected to reduce the nutrient throughflow.

4.2 Effects of farm set-ups on the environment

4.2.1 Effect of the extent of seaweed farms

Our model results show that the spatial extent of the seaweed production farms is a major driver for the intensity of decrease in winter nutrient concentrations and in phytoplankton primary production. Indeed, when upscaling seaweed cultivation to all designated OWF areas (S-C1), the highest impact occurs within the IJmuiden-Ver OWF area, which is by far the largest. On the contrary, when simulating farms of equal size in each OWF designated area (S-C3), this is no longer the case.

Similarly, within the Borssele OWF area, seaweed cultivation over 25% of a ~100 km^2 plot leads to a significant decrease in spring phytoplankton primary production >1% over an area of more than 3,000 km^2 (S-C3), while, when cultivating within the same OWF but over ~0.8 km^2, the environmental impact is extremely limited.

4.2.2 Sensitivity of different farming locations

Apart from their size/capacity, the environmental effects of the seaweed farms also depend on their location. For the same farm set-up, the percentage of annual phytoplankton primary production reduction is slightly higher in areas where phytoplankton biomass is the lowest (e.g., TNWE, scenario S-F1).

However, our results also show that, for all tested locations, the individual environmental impact of farms of equal size is quite comparable. Besides the size of the farm, the most important factor to pay attention to in order to limit its environmental impact is its location with respect to other farms. For example, seaweed farming in a ~100 km^2 plot in Borssele can lead to a reduction in spring phytoplankton primary production >1% all the way North from the Wadden Islands. Installing an additional farm in the footprint area of an existing farm will lead to increased effects at that new location. Indeed, when cultivating seaweed in the OWF area HK-NW only, the local reduction in the annual phytoplankton primary production is ~2.5 times smaller than when seaweed is cultivated in all other “upstream” OWFs as well.

Finally, splitting one large farm (covering 25% of the Borssele OWF area) into smaller plots covering the same total surface area (scenarios S-F2 and S-F3) has only limited effects on the environmental effects of seaweed cultivation at such a scale. According to the results of the other scenarios, the small plots would need to be spread over a much larger area to significantly limit

the ***local*** decreases in nutrient concentrations and phytoplankton primary production. However, the integrated effect over the entire ecosystem will most likely stay unchanged.

4.3 Future model improvements

4.3.1 Improvement of the reference ecosystem model

The overestimation of P depletion during the growing period can lead to an overestimation of competition for P between the seaweed and phytoplankton species. The model results however, show that seaweed P uptake stops during the phytoplankton growing season, but structural biomass continues growing from its internal reserves, which never become limiting. This bias in the ecosystem model has therefore most likely little influence on the amount of seaweed biomass produced at the end of the production cycle.

Another point that should be kept in mind is that, in the current implementation of the model, phytoplankton dynamics are calculated daily, before all other water quality processes. That means that, when combining with seaweed dynamics, phytoplankton have priority over seaweed for nutrient uptake at each simulation time step. The competition for the use of nutrients is therefore not fully accounted for in the case of very low concentrations (here, in spring). It is possible that this reflects reality, since phytoplankton might be able to access nutrients more effectively than seaweed due to their higher surface to volume ratio per cell, but this should be validated against future observations. Using a phytoplankton simulation module that can be computed simultaneously to other processes, would be a solution. However, we decided to keep the BLOOM module, able to represent competition of different functional groups and subsequent shifts in phytoplankton C:N:P stoichiometry, and extensively applied in the North Sea, assuming that this would have little effect since maximum nutrient uptake for seaweed and phytoplankton do not occur in the same period.

4.3.2 Improvement of seaweed dynamics

As described in the methods section, nutrient uptake and storage is parameterized using recent lab measurements on North Sea species, and the model is initialized to reach realistic target yields. However, the model results in terms of total biomass dynamics (dry/weight, total frond area, etc. over time), but also of carbon and nutrient storage could not yet be validated against field data. This step is crucially needed to assure that seaweed production yield assessments are reliable. This will be picked up in future projects, when this data is available.

The results from this study lead to the impression that the structural growth of the seaweed in the model is too high in the fall/winter period. Indeed, the seaweed already utilizes internal N in the fall, when in the field it is still a young, developing sporophyte, building up its internal storage. Therefore, the seaweed does not reach its saturating uptake in the winter as expected. This could be due to the fact that, unlike external nutrient uptake, the structural growth is now parameterized based on *S. latissima* cultivated in Norway, where both water temperature and day length are lower in that period of the year. Winter growth limitation by these meteorological factors seems to be underestimated in the current version of the model.
Additionally, preliminary tests showed that, a similar model set-up and initial seaweed biomass, using the nutrient uptake parameters from Broch and Slagstad (2012) instead of those from Lubsch and Timmermans (2019) (Table 2.2) leads to seaweed production yields higher by a factor 2.4. This shows the sensitivity of the model to such parameters and the importance of determining them not only specifically for the cultivated species but also for the specific ecosystem in which it is cultivated and to which it is adapted.

It is difficult to predict what the effect of changes in the growth limitation by meteorological factors will be on the environmental footprint. With nutrient reserves being fuller at the start of spring, the N uptake in spring might be reduced and the spring N footprint slightly smaller than estimated here.

4.3.3 Additional processes

Besides calibrating and validating the current representation of seaweed dynamics, an important feature to include for a more accurate assessment of large-scale seaweed cultivation is the

feedback of farms on the water flows. At the end of the growing season, high seaweed densities lead to an increase in drag and reduction in local current velocities (Fredriksson et al. 2020). This feedback can lead to a lower turnover of nutrients through the farm, leading to stronger depletion locally, as well as within the footprint area of the farm. In future studies, we could imagine parameterizing the reduction in velocity, based on the amount of farm surface area and the seaweed density.

However, *S. latissima* takes up most of its external nutrients in the winter period, when its fronds are still relatively small (and have limited drag). In the spring, when the seaweed reaches its maximum biomass and can exert a substantial drag on currents (and nutrient fluxes), it mainly uses its internal reserves to grow, especially for P. We therefore expect that adding the feedback of seaweed fronds on the flow in the model will have a limited effect on estimated large-scale nutrient fluxes in the Dutch North Sea and spring phytoplankton primary production.

5 Conclusion

In this study, we integrated a module simulating seaweed nutrient uptake, growth and mortality dynamics into a 3D coupled hydrodynamics-water quality model of the North Sea to assess the interactions of seaweed and phytoplankton productivity with respect to nutrients and the effect of size, location and distribution of seaweed farms on seaweed production and ecological effects. Within different modelling scenarios, we tested the effect of seaweed cultivation within different OWF designated areas and at potential current/near future cultivation test sites such as the North Sea Farm and the Voordelta area.

Our results show that an upscaling of seaweed production to 25% of all Dutch designated OWF areas would have a strong impact on the ecology, with a decrease of phytoplankton production up to 30% in some areas. The effect on nutrient concentrations and phytoplankton primary production is directly related to the size of the farms. Small scale farms (plots of ~0.8 km^2) individually have a limited impact in terms of percentage decrease in nutrients and phytoplankton production. However, the locations of seaweed farms with respect to each other is a very important factor to limit the local effects on nutrient concentrations and phytoplankton primary production. In fact, while the integrated effect on the ***entire ecosystem*** will be similar for different spatial layouts (as long as local effects are such that seaweed nutrient reserves do not get depleted), setting up a seaweed farm within the footprint area of another farm will exacerbate the ***local*** effects on nutrients and phytoplankton primary production within the downstream farm.

This study shows the importance of using coupled hydrodynamic-water quality models to assess the environmental effects of seaweed cultivation at the large-scale. A crucial next step to this work is to calibrate and validate the simulated seaweed dynamics against field measurements when these are available. We tried here to use parameters as close as possible to the North Sea reality, but structural biomass seems to grow too early in the production cycle. Furthermore, adding the feedback effect of seaweed on the flow (increase in drag), would help further refining our assessments, especially given the spatial extent of the farms' footprints in terms of nutrient and phytoplankton production reduction and subsequent importance of interactions between farms.

This work is relevant to refine future assessments of the North Sea ecological carrying capacity with respect to seaweed cultivation. This however requires setting an ecologically meaningful threshold for acceptable effects.

6 References

Ærtebjerg, G, J Carstensen, K Dahl, J Hansen, K Nygaard, B Rygg, K Sørensen, et al. 2001. "Eutrophication in Europe's Coastal Waters. Topic Report 7/2001, European Environmental Agency."

Blauw, A, M Eleveld, T Prins, F Zijl, J Groenenboom, G Winter, L Kramer, et al. 2019. "Coherence in Assessment Framework of Chlorophyll a and Nutrients as Part of the EU Project 'Joint Monitoring Programme of the Eutrophication of the North Sea with Satellite Data.'"

Blauw, A N, H F J Los, M Bokhorst, and P L A Erftemeijer. 2009. "GEM: A Generic Ecological Model for Estuaries and Coastal Waters." *Hydrobiologia* 618: 175–98.

Boogaart, L Van den, J-T Van der Wal, L Tonk, O Bos, J W P Coolen, M Poelman, S A Vergouwen, L A Van Duren, Jansen H., and K Timmermans. 2020. "Geschiktheid Zeewindparken Voor Maricultuur En Passieve Visserij, Rep. No. C127/19A."

Broch, O J, and D Slagstad. 2012. "Modelling Seasonal Growth and Composition of the Kelp Saccharina latissima." *Journal of Applied Phycology* 24: 259–76.

Deltares. 2021. "D-Water Quality Process Library Description. Technical Reference Manual. Https://Content.Oss.Deltares.Nl/Delft3d/Manuals/D-Water_Quality_Processes_Technical_Reference_Manual.Pdf."

Duren, L A Van, M Poelman, H Jansen, and K Timmermans. 2019. "Een Realistische Kijk Op Zeewierproductie in de Noordzee, Rep. No. BO-43-023.03-005."

Emeis, K C, J van Beusekom, U Callies, R Ebinghaus, A Kannen, G Kraus, I Kröncke, et al. 2015. "The North Sea - A Shelf Sea in the Anthropocene." *Journal of Marine Systems* 141: 18–33.

Fredriksson, D. W., T. Dewhurst, A. Drach, W. Beaver, A. T. St. Gelais, K. Johndrow, and B. A. Costa-Pierce. 2020. "Hydrodynamic Characteristics of a Full-Scale Kelp Model for Aquaculture Applications." *Aquaculture Engineering* 90: 102086.

Kaaij, T van der, T van Kessel, T Troost, L A van Duren, and M T Villars. 2017. "Modelondersteuning MER Winning Suppletie- En Ophoogzand Noordzee 2018 – 2027; Modelvalidatie 1230888-002."

Kooijman, S A L M. 2010. *Dynamic Energy Budget Theory for Metabolic Organization (3rd Edition)*. Cambridge University Press, Great Britain.

Los, F J, and J J Brinkman. 1988. "Phytoplankton Modelling by Means of Optimization: A 10-Year Experience with BLOOM II." *Verhandlungen Der Internationalen Vereinigung Für Theoretische Und Angewandte Limnologie* 74: 790–95.

Los, F J, M T Villars, and M W M der Tol. 2008. "A 3-Dimensional Primary Production Model (BLOOM/GEM) and Its Applications to the (Southern) North Sea (Coupled Physical–Chemical–Ecological Model)." *Journal of Marine Systems* 74: 259–94.

Lubsch, A, and K R Timmermans. 2019. "Uptake Kinetics and Storage Capacity of Dissolved Inorganicphosphorus and Corresponding Dissolved Inorganic Nitrate Uptake in Saccharina latissima and Laminariadigitata (Phaeophyceae)." *Journal of Phycology* 55 (3): 637–50.

Prins, T C, X Desmit, and J G Baretta-Bekker. 2012. "Phytoplankton Composition in Dutch Coastal Waters Responds to Changes in Riverine Nutrient Loads." *Journal of Sea Research* 73: 49–62.

Schueder, R, and L A van Duren. 2019. "First Version of IMTA Model Focused on the North Sea - IMPAQT Deliverable 3.2."

Troost, T A, J Wijsman, S Saraiva, and V Freitas. 2010. "Modelling Shellfish Growth with Dynamic Energy Budget Models: An Application for Cockles and Mussels in the Oosterschelde (Southwest Netherlands)." *Philosophical Transactions of The Royal Society B Biological Sciences* 365 (1557): 3567–77.

Vilmin, L, and L van Duren. 2019. "First North Sea IMTA Model Applications and Up-Scaling Scenario - IMPAQT Deliverable 3.4."

Zijl, F, J Groenenboom, and S C Laan. 2020. "Development of a 3D Model for the NW European Shelf (3D DCSM-FM). Report 11205259-015-ZKS-0001."

Zijl, F, S C Laan, A Emmanouil, V T M van Zelst, T van Kessel, L M Vilmin, and L A van Duren. 2021. "Potential Ecosystem Effects of Large Upscaling of Offshore Wind in the North Sea. Final Report Model Scenarios. 11203731-004-ZKS-0015."

Zijl, F, J Veenstra, and J Groenenboom. 2018. "The 3D Dutch Continental Shelf Model - Flexible Mesh (3D DCSMFM) : Setup and Validation. 1220339."

A Equations of the MALG module

Table A.1: Differential equations of state variables, process rate formulations and parameters used for the representation of Saccharina latissima in MALG. T = temperature (°C), I = radiation in water column (W/m²), dt = calculation timestep.

Differential equations for state variables
$\frac{\mathbf{dMALS}}{\mathbf{dt}} = \boldsymbol{\mu} \cdot \mathbf{MALS} - \boldsymbol{\omega} \cdot \mathbf{MALS} - \frac{\mathbf{can_{MALS}}}{(\mathbf{C:DW})_{\mathbf{MALS}}} - \mathbf{hrv} \cdot \mathbf{MALS}$
$\frac{\mathbf{dMALC}}{\mathbf{dt}} = (\mathbf{1} - \mathbf{exud}) \cdot \mathbf{pr_{MALC}} - \mathbf{resp_{MALC}} - (\mathbf{C:DW})_{\mathbf{MALS}} \cdot \boldsymbol{\mu} \cdot \mathbf{MALS} - \mathbf{hrv} \cdot \mathbf{MALC}$
$\frac{\mathbf{dMALN}}{\mathbf{dt}} = \mathbf{upt_{NH4}} + \mathbf{upt_{NO3}} - (\mathbf{N:C})_{\mathbf{MALS}} \cdot (\mathbf{C:DW})_{\mathbf{MALS}} \cdot \boldsymbol{\mu} \cdot \mathbf{MALS} - \mathbf{hrv} \cdot \mathbf{MALN}$
$\frac{\mathbf{dMALP}}{\mathbf{dt}} = \mathbf{upt_P} - (\mathbf{P:C})_{\mathbf{MALS}} \cdot (\mathbf{C:DW})_{\mathbf{MALS}} \cdot \boldsymbol{\mu} \cdot \mathbf{MALS} - \mathbf{hrv} \cdot \mathbf{MALP}$
$\frac{\mathbf{dNH4}}{\mathbf{dt}} = -\mathbf{fr_{NH4}} \cdot \mathbf{upt_N} + \mathbf{can_{MALS}} \cdot (\mathbf{N:C})_{\mathbf{MALS}}$
$\frac{\mathbf{dNO3}}{\mathbf{dt}} = -(\mathbf{1} - \mathbf{fr_{NH4}}) \cdot \mathbf{upt_N}$
$\frac{\mathbf{dPO4}}{\mathbf{dt}} = -\mathbf{upt_P} + \mathbf{can_{MALS}} \cdot (\mathbf{P:C})_{\mathbf{MALS}}$
$\frac{\mathbf{dPOC}}{\mathbf{dt}} = (\mathbf{C:DW})_{\mathbf{MALS}} \cdot \boldsymbol{\omega} \cdot \mathbf{MALS}$
$\frac{\mathbf{dPON}}{\mathbf{dt}} = (\mathbf{N:C})_{\mathbf{MALS}} \cdot (\mathbf{C:DW})_{\mathbf{MALS}} \cdot \boldsymbol{\omega} \cdot \mathbf{MALS}$
$\frac{\mathbf{dPOP}}{\mathbf{dt}} = (\mathbf{P:C})_{\mathbf{MALS}} \cdot (\mathbf{C:DW})_{\mathbf{MALS}} \cdot \boldsymbol{\omega} \cdot \mathbf{MALS}$
$\frac{\mathbf{dOXY}}{\mathbf{dt}} = \mathbf{2.67}\,(\mathbf{pr_{MALC}} - \mathbf{resp_{MALC}} - \mathbf{can_{MALS}}) + \mathbf{4.571}\,\mathbf{upt_{NO3}}$

Process rate equations

Notation	Unit	Description	Equation
$\boldsymbol{\mu}$	/day	Growth rate of MALS	$\mu = \mu_{max} \cdot f(A) \cdot f(T) \cdot f(n) \cdot \min(f(N), f(P), f(C))$
$\mathbf{f(A)}$	-	Size limitation factor for growth	$f(A) = m_1 \cdot e^{-\left(\frac{A}{A_0}\right)^2} + m_2$
$\mathbf{f(T)}$	-	Temperature limitation factor for growth	$f(T) = \begin{cases} 0.08\,T + 0.2 & \text{for} \quad -1.8 \le T < 10 \\ 1 & \text{for} \quad 10 \le T \le 15 \\ \frac{19 - T}{4} & \text{for} \quad 15 < T \le 19 \\ 0 & \text{for} \quad 19 < T \end{cases}$
$\mathbf{f(n)}$	-	Photoperiod limitation factor for growth	$f(n) = a_1\left(1 + \text{sign}(\lambda(n)) \cdot \sqrt{\lvert\lambda(n)\rvert}\right) + a_2$ where: $\lambda(n) = \frac{dl(n) - dl(n-1)}{\max(dl)}$ dl is the daylength and n is the Julian day
$\mathbf{f(X)}$ $\mathbf{X} \in [\mathbf{N}, \mathbf{P}]$	-	Nutrient (stores) limitation factor growth	$f(X) = 1 - \frac{MALX_{min}}{MALX}$
$\boldsymbol{\omega}$	/day	Erosion/mortality rate of MALS	$\omega = \frac{10^{-6} \cdot e^{\varepsilon \cdot A}}{1 + 10^{-6} \cdot (e^{\varepsilon \cdot A} - 1)}$

$\mathbf{upt_X}$ $\mathbf{X \in [N, P]}$	gX/day	Uptake of dissolved inorganic nutrients for build-up of MALX	$\mathrm{upt_X} = \frac{\mathrm{MALS}}{(\mathrm{DW:A})_{\mathrm{MALS}}} \cdot \frac{\mathrm{MALX_{max}} - \mathrm{MALX}}{\mathrm{MALX_{max}} - \mathrm{MALX_{min}}} \cdot \frac{\mathrm{DIX}}{\mathrm{K_X} + \mathrm{DIX}} \cdot \mathrm{J_{X,max}}$
$\mathbf{fr_{NH4}}$	-	Fraction of NH4 in DIN uptake	$\mathrm{fr_{NH4}} = \frac{\mathrm{NH4}}{\mathrm{NO3} + \mathrm{NH4}}$
$\mathbf{pr_{MALC}}$	gC/day	Primary production rate	$\mathrm{pr_{MALC}} = \mathrm{A} \cdot \mathrm{P_S(T)} \cdot \left[1 - e^{\frac{\alpha \cdot \mathrm{I}}{\mathrm{P_S(T)}}}\right] \cdot e^{\frac{\beta \cdot \mathrm{I}}{\mathrm{P_S(T)}}}$ where: $\mathrm{P_S(T)} = \frac{\alpha \cdot \mathrm{I_0}}{\ln\left(1 + {}^{\alpha}/_{\beta}\right)}$
$\mathbf{resp_{MALC}}$	gC/day	Respiration rate	$\mathrm{resp_{MALC}} = \max\left(\mathrm{resp_{MALC,max}}, \mathrm{MALC/dt}\right)$ where: $\mathrm{resp_{MALC,max}} = \mathrm{A} \cdot \mathrm{R_1} \cdot e^{\left(\frac{\mathrm{Tar}}{\mathrm{Tr1}} - \frac{\mathrm{Tar}}{\mathrm{T+273.0}}\right)}$
$\mathbf{can_{MALS}}$	gC/day	"Cannibalization" rate: use of C in structural mass for respiration if MALC is depleted	$\mathrm{can_{MALS}} = \mathrm{resp_{MALC,max}} - \mathrm{resp_{MALC}}$
hrv	/day	Harvest rate	0.

Description of parameters

Notation	Unit	Description
$\mathbf{(DW:A)_{MALS}}$	gDW/m^2	Dry weight to surface area ratio of seaweed leaf
$\mathbf{(C:DW)_{MALS}}$	gC/gDW	C:DW ratio of MALS
$\mathbf{(N:C)_{MALS}}$	gN/gC	N:C ratio of MALS
$\mathbf{(P:C)_{MALS}}$	gP/gC	P:C ratio of MALS
$\mathbf{\mu_{max}}$	/day	Maximum growth rate of MALS
$\boldsymbol{A_0}$	m^2	Frond area growth limitation parameter
$\mathbf{m_1}$	-	Frond area growth limitation adjustment parameter
$\mathbf{m_2}$	-	Frond area growth limitation adjustment parameter
$\mathbf{a_1}$	-	Photoperiod limitation parameter
$\mathbf{a_2}$	-	Photoperiod limitation parameter
$\mathbf{I_0}$	W/m^2	Optimum light intensity for photosynthesis
$\boldsymbol{\alpha}$	gC/(W.day)	Photosynthetic efficiency
$\boldsymbol{\beta}$	gC/(W.day)	Light inhibition parameter
$\boldsymbol{\varepsilon}$	m^{-2}	Frond mortality parameter
exud	-	Exudation fraction (proportion of photosynthesis not assimilated into MALC)
$\mathbf{MALN_{min}}$	gN/gDW	Minimum N storage with respect to MALS
$\mathbf{MALN_{max}}$	gN/gDW	Maximum N storage with respect to MALS
$\mathbf{K_N}$	gN/m^3	Half-saturation coefficient for DIN uptake
$\mathbf{J_{N,max}}$	gN/m^2/day	Maximum DIN uptake rate
$\mathbf{MALP_{min}}$	gP/gDW	Minimum P storage with respect to MALS

$\mathbf{MALP_{max}}$	gP/gDW	Maximum P storage with respect to MALS
$\mathbf{K_P}$	gP/m^3	Half-saturation coefficient for DIP uptake
$\mathbf{J_{P,max}}$	gP/m^2/day	Maximum DIP uptake rate
$\mathbf{R_1}$	gC/m^2/day	Reference respiration rate at Tr1
Tar	K	Arrhenius temperature for respiration
Tr1	K	Reference temperature for respiration

B Absolute differences in spring nutrient concentrations and phytoplankton primary production between simulated scenarios and reference runs

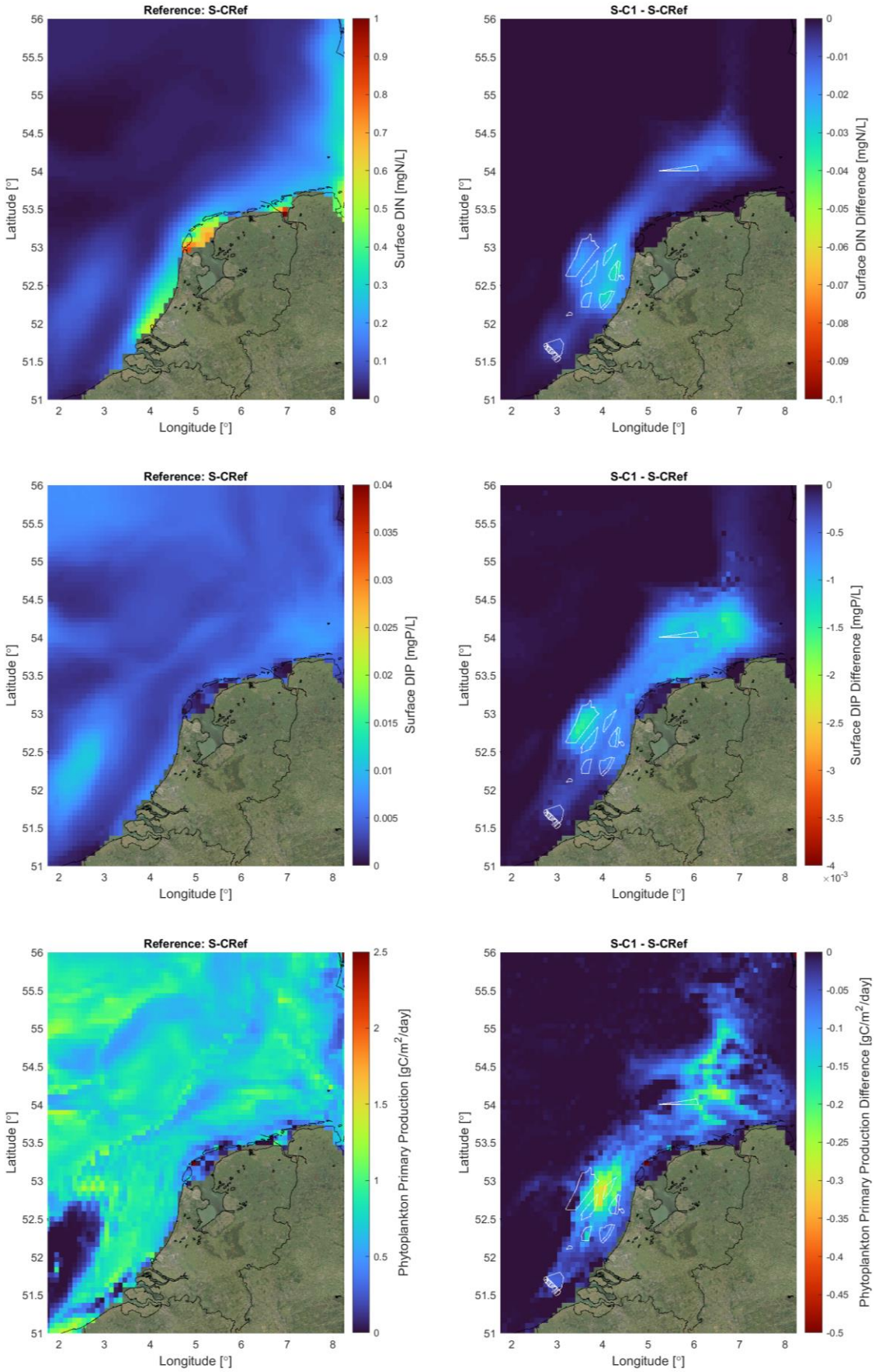

Figure B.1: Effect of seaweed cultivation over 25% of all designated OWF areas (scenario S-C1) on spring nutrient concentrations and phytoplankton primary production. Top: surface DIN. Middle: surface DIP. Bottom: Phytoplankton primary production. Left: concentrations in reference simulation. Right: absolute difference between scenario run and reference.

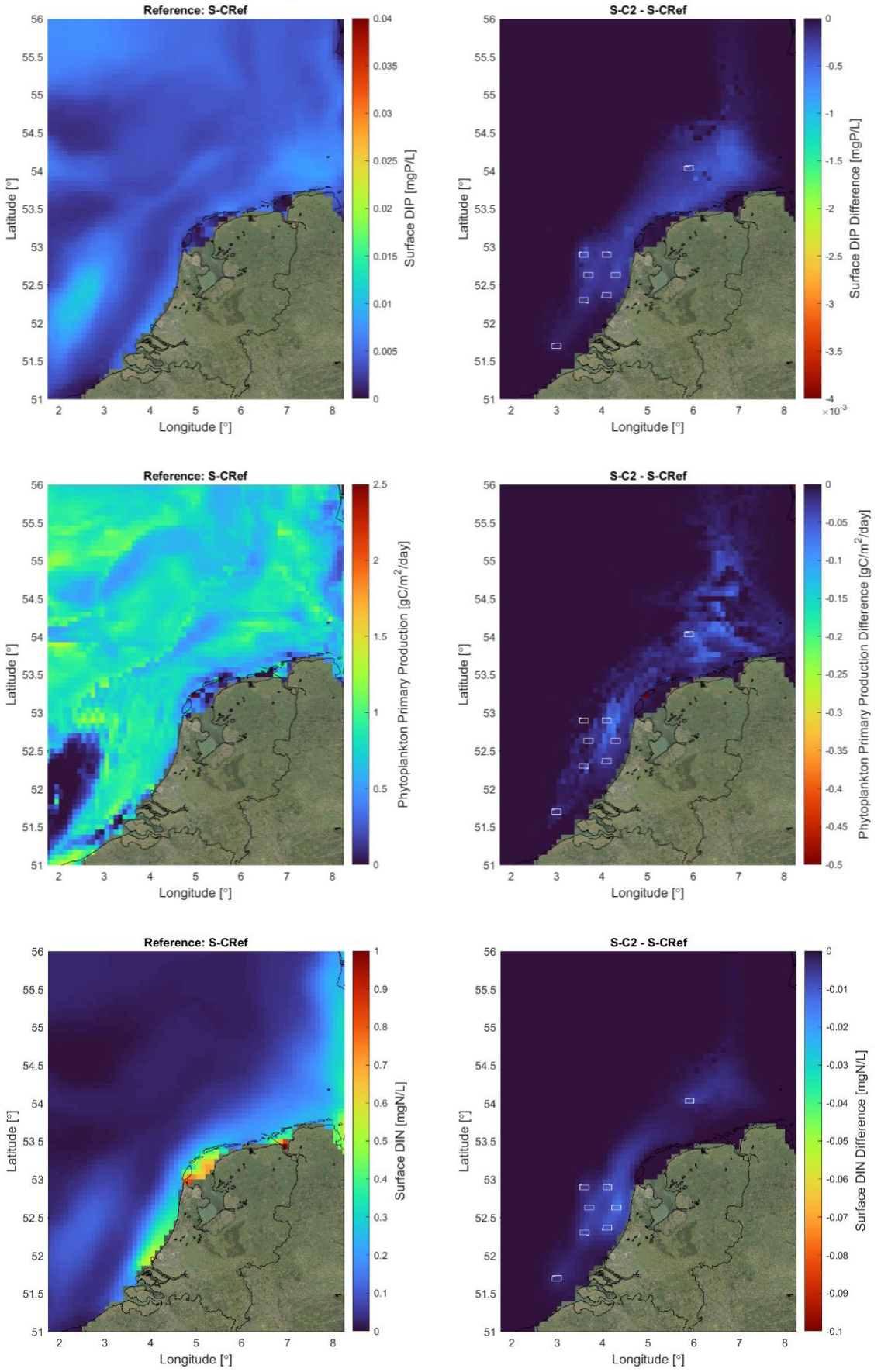

Figure B.2: Effect of seaweed cultivation over 25% of ~100 km^2 patches in OWF areas (scenario S-C2) on spring nutrient concentrations and phytoplankton primary production. Top: surface DIN. Middle: surface DIP. Bottom: Phytoplankton primary production. Left: concentrations in reference simulation. Right: absolute difference between scenario run and reference.

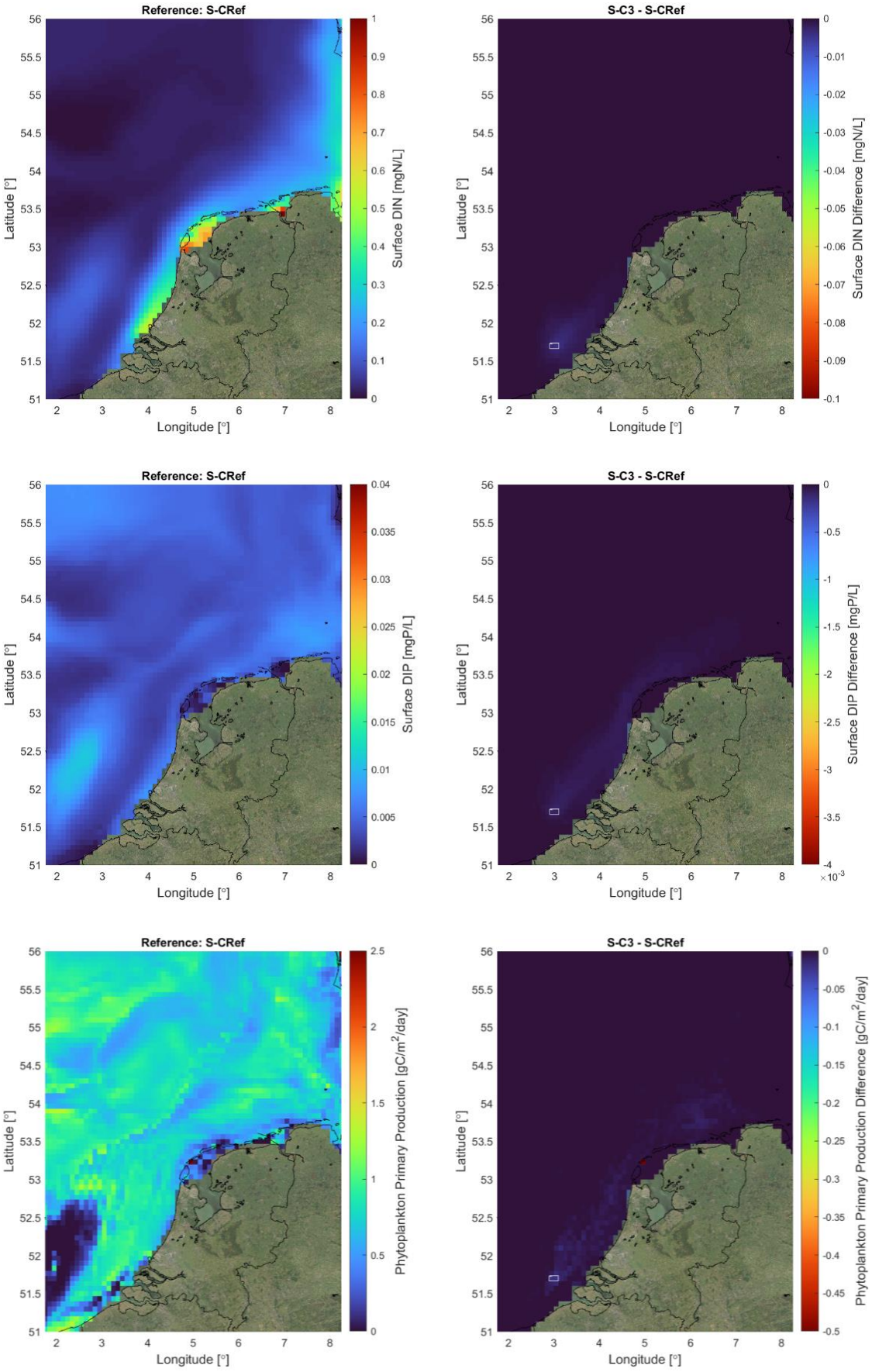

Figure B.3: Effect of seaweed cultivation over 25% of a ~100 km^2 patch in the Borssele windfarm area (scenario S-C3) on spring nutrient concentrations and phytoplankton primary production. Top: surface DIN. Middle: surface DIP. Bottom: Phytoplankton primary production. Left: concentrations in reference simulation. Right: absolute difference between scenario run and reference.

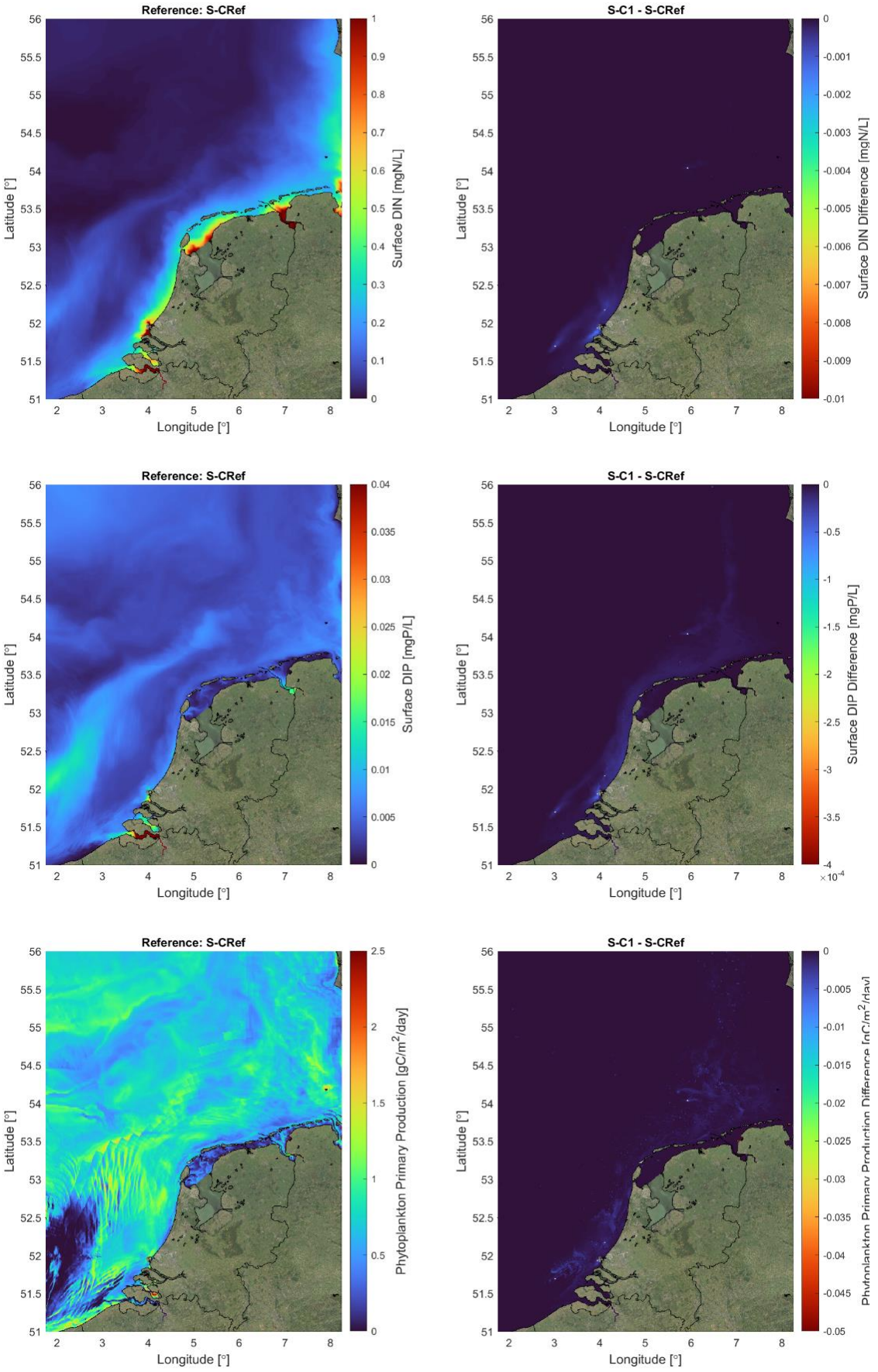

Figure B.4: Effect of seaweed cultivation 1-cell farms (~0.8 km^2) in Borssele, the NSF, Voordelta and TNWE (scenario S-F1) on spring nutrient concentrations and phytoplankton primary production. Top: surface DIN. Middle: surface DIP. Bottom: Phytoplankton primary production. Left: concentrations in reference simulation. Right: absolute difference between scenario run and reference.

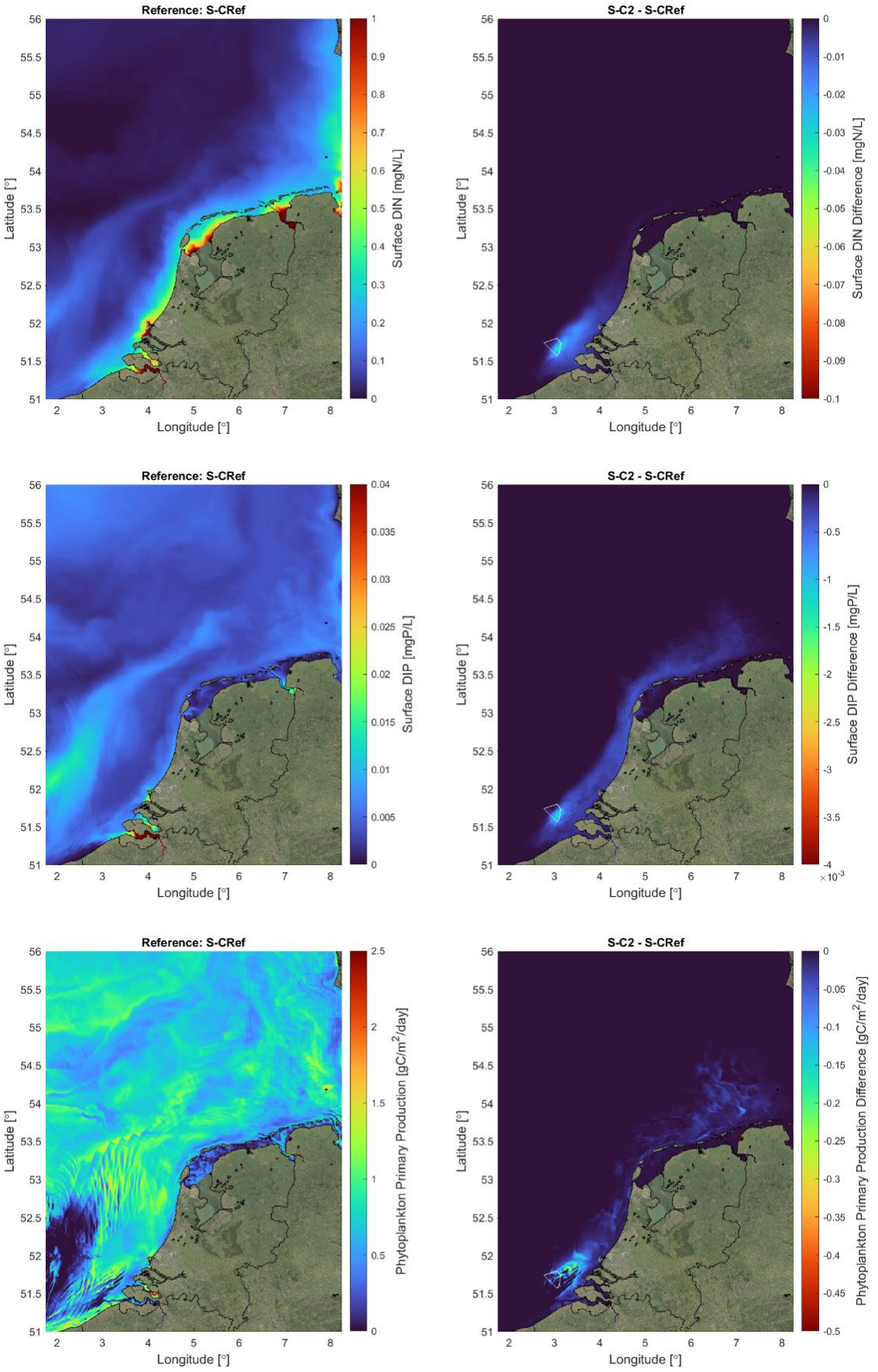

Figure B.5: Effect of seaweed cultivation in one large farm covering 25% of Borssele OWF area (scenario S-F2) on spring nutrient concentrations and phytoplankton primary production. Top: surface DIN. Middle: surface DIP. Bottom: Phytoplankton primary production. Left: concentrations in reference simulation. Right: absolute difference between scenario run and reference.

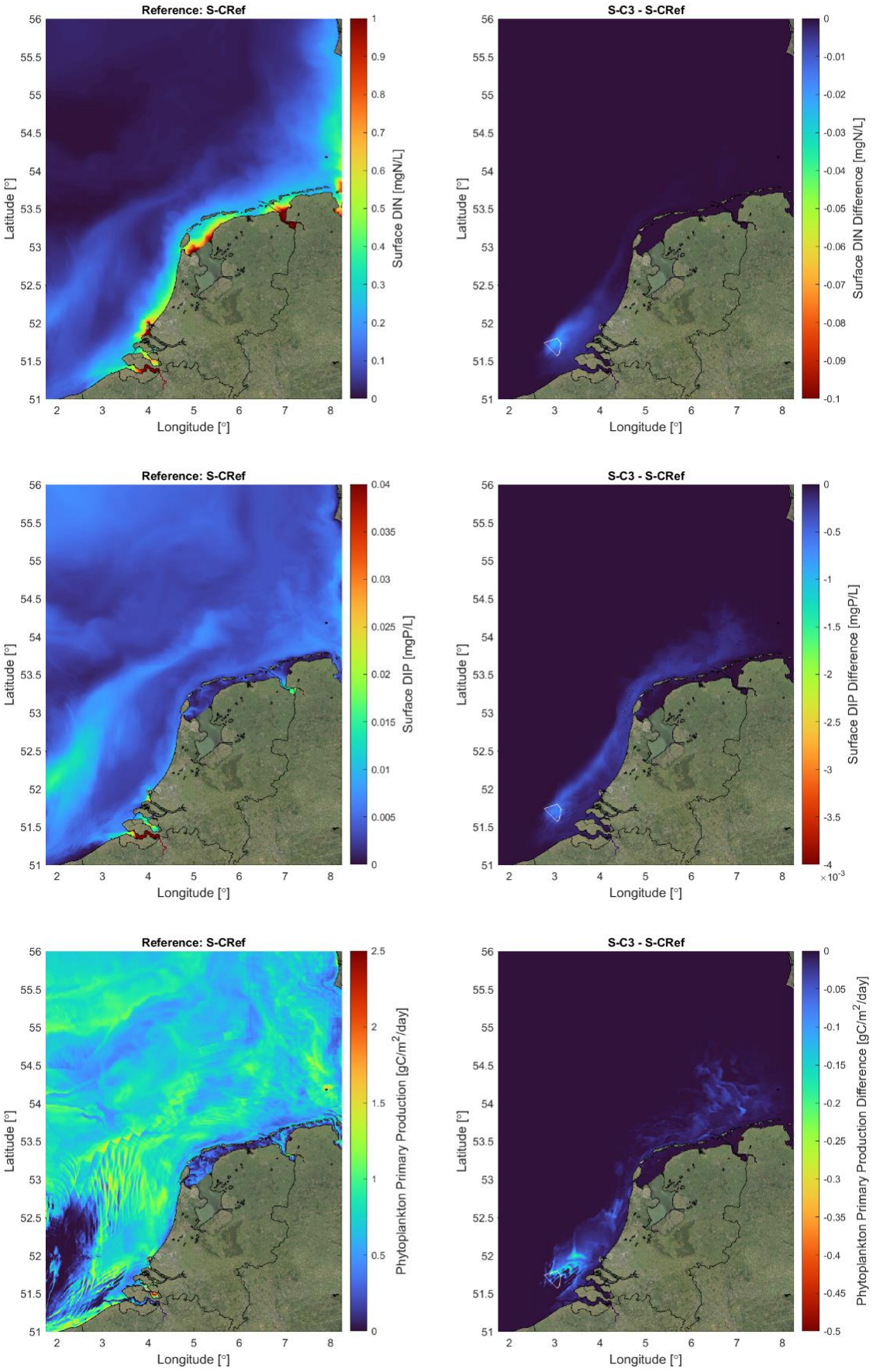

Figure B.6: Effect of seaweed cultivation in 107 1-cell farms covering 25% of Borssele OWF area (scenario S-F3) on spring nutrient concentrations and phytoplankton primary production. Top: surface DIN. Middle: surface DIP. Bottom: Phytoplankton primary production. Left: concentrations in reference simulation. Right: absolute difference between scenario run and reference.

Deltares is an independent institute for applied research in the field of water and subsurface. Throughout the world, we work on smart solutions for people, environment and society.

Deltares

www.deltares.nl

Handtekening: 

E-mail: luca.vanduren@deltares.nl

Handtekening: 

E-mail: jos.vangils@deltares.nl

Handtekening: 

E-mail: paul.saager@deltares.nl